SPECIAL REPORT No. 88

PRELIMINARY FULL-SCALE WIND-TUNNEL INVESTIGATION OF WING DUCTS FOR RADIATORS

By Abe Silverstein and F. R. Nickle
Langley Memorial Aeronautical Laboratory

March 1938

NATIONAL ADVISORY COMMITTEE FOR AERONAUTICS

PRELIMINARY FULL-SCALE WIND-TUNNEL INVESTIGATION OF WING DUCTS FOR RADIATORS

By Abe Silverstein and F. R. Nickle

INTRODUCTION

Wing ducts for liquid-cooled engine radiators have been investigated in the N.A.C.A. full-scale wind tunnel on a large model airplane. The tests were made to determine the relative merits of several types of duct and radiator installations for an airplane of a particular design. Definite specifications were given regarding the quantity of air required to flow through the Prestone and oil radiator at the different flight conditions and the program of tests was principally arranged to satisfy these particular air-flow requirements with a minimum of adverse effects on the aerodynamic characteristics of the airplane. In the test program the principal duct dimensions were systematically varied, and the results are therefore somewhat applicable to the general problem of wing duct design, although they should be considered as preliminary and only indicative of the inherent possibilities.

Conventional airplanes with liquid-cooled engines are ordinarily equipped with cowled underslung radiators. The high-speed drag of these installations has been shown to be as much as 15 to 20 percent of that of the entire airplane. Recent studies have indicated advantages in using expanding ducts with large radiators located at the low velocity sections of the ducts. The power absorbed by the radiator is a function of the velocity through the core, and reduction of the core velocity markedly decreases the radiator losses. The net gain from using an expanding duct on external radiators, however, is less than indicated from consideration of the core losses alone since a heavier radiator with a larger frontal area is required which increases both the induced and interference drag. In the present tests the expanding ducts have been located either wholly or partially within the wing in an attempt to reduce the interference drag between the duct and the remainder of the airplane and to reduce the exposed frontal area. The passage of air through expanding ducts inevitably introduces energy losses at the inlet, in the expansion along the duct, at the duct walls, and a

further loss at the outlet. The magnitude of the advantage to be realized by the use of the expanding ducts depends therefore on the extent to which these losses may be reduced.

The important requirements for satisfactory wing cooling ducts are summarized as follows:

1. Sufficient cooling air provided to the radiators for all flight conditions.

2. Low cooling drag at high speed.

3. Small adverse effects on the maximum wing lift.

This report presents the results of over 100 tests conducted with numerous duct-radiator combinations on a two-engine pusher-type model airplane arranged as a mid-wing monoplane. Test data include measurements of the quantity of air flowing through the ducts and the effect of the ducts on the aerodynamic characteristics of the airplane. The tests include Prestone radiator installations entirely within the wing and in external cowlings along the lower wing surface; combinations of Prestone and oil radiators in ducts entirely within the wing; and Prestone radiators in wing ducts with cowled oil radiators partly exposed at several positions along the lower wing surface. The various design parameters such as duct size and location were varied in a systematic manner. The effect of the pressure drop through the radiator on the duct performance was investigated for several of the combinations.

Owing to the structural arrangements in the full-size airplane which were simulated in the model, it was not possible to design the model ducts in an optimum manner to minimize the internal losses. The web members of both the front and rear spars passed through the duct, and it was necessary in some cases to bend the duct rather sharply to avoid the spar flange members. An ideal design could largely eliminate these structural difficulties, and it is therefore believed that the preliminary results of this investigation are of greater interest as an indication of the possibilities inherent in the internal wing duct system rather than as exact quantitative data for an optimum design. A systematic test program is now in progress at the N.A.C.A. laboratory on improved wing arrangements to obtain data more applicable for general design purposes.

DESCRIPTION OF DUCTS AND RADIATORS

The model tested was arranged as a two-engine mid-wing monoplane having a wing span of 35 feet and a wing area of 172 square feet. The wing was tapered in plan form and section, and the wing profiles are of the N.A.C.A. 230 family with the middle of the radiator duct approximately at an N.A.C.A. 23017 section. The duct dimensions are given as a percentage of the reference wing chord of 66.65 inches. To expedite the test, the ducts and radiators were installed only in one side of the model. The effects of the radiator and ducts for both engines were considered to be double those obtained for the one.

For all the tests with the Prestone radiator within the wing the location of the radiator, the 15-inch duct width, and the most forward location of the duct outlet were maintained constant. These dimensions were dictated by the space available in the model. The variables consisted in the size of the duct inlet and outlet and their chordwise location.

The principal dimensions of all the test arrangements are given in table I. The tests have been grouped together under arrangements designated A, B, C, etc. Tests grouped under each arrangement have the same general family characteristics with the variations within each group largely consisting of changes in the detail dimensions. The various nose inlets for the ducts are dimensioned in figure 1. To facilitate the description of the various ducts two numbers are used to designate each of the duct inlets and outlets. For example, a sample designation for the Prestone duct may be inlet 45, outlet 36 in which:

1. The first number 4 of the inlet pair gives the approximate percentage of the inlet opening dimension to the wing chord.

2. The second number 5 gives the approximate percentage location of the center of the inlet behind the nose reference in terms of the wing chord.

3. The number 3 at the beginning of the outlet group indicates the approximate percentage opening of the outlet in terms of the wing chord.

4. The last number 6 (x 10) indicates that the outlet is about 60 percent of the wing chord behind the nose. For the cases in which the outlet is at the flap, the flap delfections define the opening.

In designing the ducts, reference was made to the theoretical pressure distribution around an airfoil section similar to the N.A.C.A. 23017. It was indicated from this that the optimum pressure differences for inducing a flow through the wing could be obtained by placing the inlet at the nose stagnation point and the outlet near the 20-percent-chord point on the upper surface. Space restriction prevented the location of the outlet further forward than about the 55-percent-chord point; so this was chosen as the most satisfactory preliminary location for the outlet (arrangement A, table IA). In subsequent tests the outlets were moved progressively rearward to approximately 70- and 80-percent-chord locations (arrangements B, C, D, E, F), and finally to the opening formed by deflecting the split trailing-edge flaps (arrangement G).

The inlets for arrangement A were varied so as to cover openings whose centers varied from 1 to 6 percent back from the reference at the nose. This reference point is defined by the intersection of the chord line with the section profile. Tuft observations made on the 23017 airfoil show that the front stagnation point varies from about directly at the reference for the high-speed condition to about 1.75 percent behind this point for the climbing attitude.

Arrangement H was provided with outlet flaps of two types designated as style A and B as shown on figure 2. The flaps were varied through an angle range of from 15° to 45°. Arrangement I was fitted with scoops at the inlet which were adjustable from 30° to 45° with the chord line. Center-hinged flaps were utilized in arrangement J to control the flow through the outlet. In arrangement K the Prestone radiator was enclosed in an external cowling which was adjustable to several different distances from the lower wing surface. Flaps and scoops were also provided to control the flow at the outlet and inlet, respectively. In arrangement L both the Prestone and oil radiators were completely enclosed within the wing with the flow through the nose inlet divided so that about one-fourth of the air passed through the oil radiator and three-fourths through the Prestone radiator. Arrangement

M was a variation of L differing in that a separate inlet with a scoop was provided on the lower surface to supply air to the oil radiator. In both cases center-hinged outlet flaps were provided. The oil radiators were located in a cowled duct on the lower wing surface for arrangements N and P. The centers of the oil radiators were at approximate distances of 30 and 65 percent from the leading edge, respectively. The duct in both cases was provided with an outlet flap, and duct P was designed to retract into the wing. The Prestone radiator for both these rangements was located within the wing with the duct combination of inlet 55 and exit 56.

Two types of Prestone radiators designated as cores A and B have been tested in the ducts. (See fig. 3.) Radiator A is a fine-mesh fin-type core, 4 inches deep and 9-3/8 by 14-7/16 inches in cross section. This core was used in arrangements A to I, inclusive. Radiator B is a standard Air Corps, hexagonal-tube, cartridge-core type, 9 inches deep and 8-1/16 by 15-3/8 inches in cross section and was used in arrangements J to P. The oil cooler consisted of two circular radiators 4-1/2 inches in diameter and 7 inches long with the same type of tubes as radiator B. To simulate radiators of higher pressure drops, metal screens of 16 and 40 mesh were added to the face of radiator A for certain of the tests. The pressure drops through the Prestone radiator cores both with and without screens are shown in figure 4 over a range of velocities representative of those occurring in the ducts.

TESTS

A general summary of the tests is given in table II. Measurements were made of the lift and drag of the model, the quantity of air flowing through the duct, and the pressure drop across the radiator. The quantity of air flow was obtained simply as a product of the air velocity through the duct and the area of the duct section. These data were obtained in most cases over the entire range of flying attitudes of the airplane. The equipment and procedure for the force measurements are described in reference 1.

The velocity of the air through the duct was measured by means of total-head tubes and static orifices.

For the preliminary tests A1 to A22, eight total-head tubes were used to survey the duct area; for the remainder of the Prestone radiator tests, to obtain higher accuracy, the number of tubes was increased to 16. Owing to the poor distribution of flow in the ducts, the air quantities and velocities determined by means of the 8- and 16-tube measurements failed to agree within about 10 percent; obviously the later values obtained with the larger number of tubes are the more reliable. The static pressures in front of and behind the radiator were measured by means of flush orifice-type static openings at the sides of the duct and a single row of static tubes located at the center of the duct in front of the radiators. A similar system of velocity measurement was employed in the oil radiator ducts. The air pressures were carried from the model to the test-chamber floor through copper and rubber tubing where they were measured with standard N.A.C.A. micromanometers.

Drag and air-flow measurements were obtained for all the duct arrangements at a tunnel velocity of 60 miles per hour. Some of the more promising combinations were tested both at 60 and at 100 miles per hour to study scale effect.

RESULTS AND DISCUSSION

A summary of the final results is given in table II where the tests are grouped as in table I. The results which are presented include the percent change in the airplane drag that may be attributed to each duct installation at the high-speed and climb conditions, the increment of change in the airplane maximum lift coefficient, the quantity of air flowing through the radiator duct at the high-speed and climb attitudes, and the over-all duct efficiency. A close study of the test results discloses may disturbing and unexplainable irregularities which preclude an exact quantitative discussion. The results show in a qualitative way the effect of varying the important duct parameters upon the duct efficiency and upon the over-all airplane characteristics.

The air measurements are in general believed to be accurate within ±10 percent, although for several cases in which separation of the flow from the duct walls occurred the error may be higher. The relatively low pre-

cision is attributed to the irregular velocity distribution in the duct with the subsequent measuring difficulties (figs. 5 and 6). Part of the dissymmetry is caused by the tubular front spar of the model which passes through the duct and whose wake is clearly outlined by the measurements, and part is due to the engine nacelles which lowered the velocity on the inboard side of the duct at high angles of attack. These difficulties are peculiar to the model tested and may be eliminated; however, further irregularities in the vertical velocity distribution due to the rapid pressure changes over the nose of the wing seem inherent for inlets close to the leading edge.

The drag changes are believed to be accurate to within ±2 percent, i.e., increments in drag tabulated as 10 percent may with equal precision be 8 or 12 percent. The precision of the drag measurements was reduced by the necessity for doubling the measurements made with cooling ducts on one side of the model only.

The drag increments and air quantities are tabulated at lift coefficients of 0.15 and 0.70 which correspond respectively to the high-speed and climb conditions. The drag increments have been given as percentages of the complete airplane drag without a radiator installation.

These reference drag values for the complete airplane at the afore-mentioned lift coefficients are as follows:

Lift coefficient C_L	Test velocity V m.p.h.	Drag coefficient C_D
0.15	60	0.0291
.15	100	.0280
.70	60	.0785
.70	100	.0755

The difference between the drag coefficients for the two tunnel velocities is attributed to scale effect.

The effects of the radiator ducts on the maximum

lift coefficients are shown as increments in lift coefficient rather than as percentages. Both the drag and lift changes are presented for installation of two ducts on the model, although as previously mentioned, the test data were obtained from a single duct installation. The air-flow measurements at the lift coefficients for high speed and climb have been given, however, for a single radiator-duct installation, and the results for both the 60- and 100-mile-an-hour tests have been adjusted to an airplane velocity of 100 miles per hour. To a first approximation the quantity of air flow for an air speed of 200 miles per hour will simply be twice that given in the table, etc.

The last column in the table presents values of the duct efficiency in the high-speed attitude. Duct efficiency is defined as the ratio of the useful work done to the total work expended in the radiator duct system. The useful work is that required to force the cooling air through the radiator core and is equal to the quantity of air flowing multiplied by the pressure drop through the radiator. The pressure drops as shown in figure 4 were used in these computations. The total work expended on the system is equal to the added drag due to the radiator-duct installations multiplied by the velocity of flight. The duct efficiency may therefore be derived as follows:

$$\eta = \frac{Q \ \Delta P}{\frac{1}{2}\rho \frac{V^3}{3600} \Delta C_D \ S}$$

Since

$$\Delta P = \frac{1}{2}\rho \frac{V_R^2}{3600} \Delta p$$

$$\eta = \frac{Q \ \Delta p \ V_R^2}{\Delta C_D \ S \ V^3}$$

Since

$$V_R = \frac{Q}{A}$$

then

$$\eta = \frac{Q^3 \Delta p}{\Delta C_D \; S \; A^2 V^3}$$

in which

η is duct efficiency

ΔC_D, increment of drag coefficient due to ducts and radiators (1 radiator)

S, wing area

A, radiator area

ΔP, pressure drop through radiator in pounds per square foot

Δp, ratio of the pressure drop through radiator core to the dynamic pressure at the face of the radiator (not to be confused with the dynamic pressure of the free stream - see fig. 4)

Q, quantity of air flow in cubic feet per minute (1 radiator)

V, free stream velocity, feet per minute

V_R, velocity at face of the radiator

CHARACTERISTICS OF INTERNAL DUCT ARRANGEMENTS

The following paragraphs show the dependence of the duct performance upon the principal duct dimensions and arrangement. The discussion relates particularly to the effects of the ducts on the high-speed drag and the quantity of air delivered. In general, for all the better internal duct arrangements tested, the maximum lift coefficient was not appreciably changed by the duct and in many cases the lift was slightly increased. The increase in lift is attributed to the favorable effect of the outlet flow on the boundary layer on the upper surface of the wing.

Effect of inlet size.- Figures 7 to 11 inclusive indicate the effect of varying the inlet width along the chord upon the quantity of air flow for several internal duct combinations. In the design of the duct inlets it became obvious that it would be impossible to change the duct width without changing the effective duct position. By holding the dimension "B" (see fig. 1) at the center of the inlet constant, and increasing the equal amounts on either side of the inlet center line, the results shown on figures 7, 8, and 9 were obtained, whereas if the dimension "A" to the front of the inlet is held constant and all the width added to the rear, the results were different as shown in figures 10 and 11. With both methods of increasing the duct width the quantity of air flow at the high-speed condition increases directly with the width of the duct inlet; however, this is true at the climb condition only when the width is added to the rear of the opening. It is to be noted on figures 8 and 9 for the tests in which "B" is held constant that the increase in flow for openings above 3-1/2 percent of the chord is negligible, whereas on figure 11 for the case where A is held constant the flow increases continuously with the width. Inasmuch as the front lip, which is located by dimension "A", is the most sensitive portion of the inlet opening to small dimension changes, it is believed that more understandable conclusions may be reached with this dimension rather than B as the reference. No definite conclusions regarding the increase in drag with increase in duct width were reached from the test results.

Effect of inlet position.- The effect of the duct inlet position on the air flow is shown in figures 12 to 15 inclusive. These data have been plotted with the dimension "A" locating the inlet position. From these results it should be noted at the high-speed lift coefficient that the air flow through the duct decreases with increasing value of A (figs. 12 and 14) whereas at the lift coefficient for climb the air-flow quantity increases with increase in this dimension (fig. 13). Extrapolation of the 100-mile-per-hour test results (fig. 14) would indicate that for inlets in which the value of A was greater than 3 percent, the flow for the high-speed condition would be negligible, whereas the 60-mile-per-hour tests with the same duct arrangements show zero flow inlet positions to be somewhat further to the rear. These data and results from the oil-cooler tests with arrangement M in which the inlet was well back along the lower

surface substantiate the observation that the rearward location of the inlet position is limited by the air-flow requirements for the high-speed condition. Accompanying the decrease in air flow at the high-speed condition with increase in the value of A is the lower value of the high-speed drag coefficient as shown on figure 15.

The test results show that the change in the quantity of air through the duct with angle of attack is primarily a function of the inlet position as is shown in figure 16. In the case of inlet 63 (see fig. 1) which is well forward with the center of the opening almost at the reference line, the quantity of air flow changes only slightly with changing angle of attack (fig. 16). As the opening is moved progressively rearward to positions 55 and 45, it is to be noted that the difference between air flow at the angles of 0° and 4° becomes increasingly greater. The flight velocity under full power conditions varies with the angle of attack and a requirement of the optimum inlet is that it should regulate the air flow to a constant amount regardless of the attitude. A simple analysis shows that the air quantities at 100 miles per hour should vary as $C_L^{1/2}$ in order for the foregoing conditions to be met. The theoretical curve with the quantity varying as $C_L^{1/2}$ is shown on figure 16 from which it may be observed that the flow for duct 55-56 has similar, although not identical, characteristics.

The results indicate generally that inlets similar to those numbered 45 and 55 are most favorable for the particular wing tested. It is to be expected that this optimum inlet location will change for other wing profiles; however, not greatly for medium-thick, nearly symmetrical airfoils such as are now in common use.

Effect of outlet size.- The effect of the outlet size on the quantity of air flow is shown in figures 17 to 20, inclusive, for several duct arrangements and lift coefficients. The results show in general that the quantity increases with the size of the outlet openings and further illustrate that the outlet opening is a vantage point at which quantity may be restricted if desired. Several extreme cases of large duct outlet were tested similar to 13 and F2 and for these cases some increase in air flow was found, but not in porportion to the amount of the upper surface opening which was utilized. The adverse effect of restricting the duct outlet size when

large air quantities are desired is aptly demonstrated by the results of duct arrangements L and M (table II) which were rendered inefficient and unsatisfactory owing to the restriction to the Prestone duct outlets caused by including the oil ducts within the wing. The greater flow with larger outlet openings is accompanied by increased drag as shown in figure 20. For cases therefore in which excessive air flow occurs at the high-speed attitude some throttling device such as a shutter should be used to reduce the flow.

Effect of outlet position.- Conclusions regarding the effects of changing the outlet position are not as well defined as those for the outlet size; however, from the results given in table II for arrangements A, B, and E, it may be noted that as the outlet is moved rearward the air-flow quantity for the same inlets shows a general tendency to decrease. This is to be expected by consideration of the pressure-distribution curves for the airfoil, since, as the outlet is moved to the rear, the pressure difference available for producing a flow through the wing is decreased. Some tests were made to determine the efficiency of duct outlets through a split flap at the trailing edge of the wing, the results of which are shown in figures 21, 22, and 23. The air flow increases only slightly with increasing flap deflection and reference to figure 23 will show that there is an attendant large increase in drag. The present measurements of the change in air flow with flap deflection are not considered particularly reliable owing to the structural restriction ahead of the flap outlets shown in table I, arrangement G.

Further research is required to determine definitely the optimum location of the outlet, although for positions aft of the 50-percent-chord station the present tests show that the location is not particularly critical.

Effect of scoops.- In an attempt to increase the air flow through the internal wing ducts at the climb condition scoops were added at the inlets. A diagram of a sample scoop is shown in figure 24. Results shown on figure 25 indicate that scoops are relatively ineffective for increasing the quantity of air flow and, in fact, large scoop deflections slightly decrease the quantity. Furthermore, the high-speed drag is greatly increased as shown in table II. Apparently the scoop acts as a spoiler on the wing and sufficiently decreases the pressure differ-

ences over the wing so as to negate the positive effect of the increased inlet area.

Effect of flaps.- External flaps of several different types as shown on figure 2 and table I were applied at the outlet of the duct in an attempt to increase the quantity of air flow. As shown on figures 26 and 27, the flaps increased the quantity of the air flow about 15 percent in several cases but with an attendant large increase in the drag at the high-speed condition. For several of the tests shown with arrangements J, L, M, N, and P, a shutter-type flap hinged at its midpoint in the center of the duct was employed. When this flap was placed with its chord axis parallel to the outlet of the duct there was no large restriction of the outlet area. In general, the results showed that flaps of this type are not particularly effective in increasing the quantity of air flow and can in some cases rather seriously increase the drag of the wing. It may be concluded that flaps which extend above the wing profile are not particularly desirable for controlling the flow in an internal duct since they are relatively ineffective for increasing the flow; and for throttling, a more efficient arrangement such as an internal flap or shutter may be employed.

Characteristics of External-Cowled Ducts

The several arrangements of external-cowled ducts with expanding passages such as K, N, and P, gave similar results. In contrast to the internal ducts, the quantity of air flowing was almost constant for all angles of attack (fig. 28). By retracting the radiator progressively into the wing, it was possible to obtain corresponding decreases in the drag for the high-speed condition. For the forward location of the radiator as in arrangement N the maximum lift coefficient was not appreciably affected by the duct; however, the rear locations K and P both contributed toward a slightly smaller maximum lift coefficient. As in the case of the internal ducts neither flaps nor scoops were particularly successful in improving the duct performance. Flaps at the exit effectively seemed to decrease the flow; however, the drag was not reduced correspondingly. Scoops increased the flow somewhat but at the cost of large increases in drag.

Efficiency of Duct Systems

The duct efficiency is perhaps the best criterion for comparison of the various duct arrangements. In the present tests, due to the fact that the spanwise duct width was not changed, it was not possible to obtain equal flows through all of the ducts, and the assumption must be made when using the duct efficiency as a criterion that both the air flow and drag will increase proportionately with increasing duct width. Internal duct arrangements, such as A10, A14, A17, and A21, gave the highest efficiencies, which varied from about 100 to over 100 percent. The efficiency values over 100 percent indicate that the flow through the duct decreased the wing profile drag by means of boundary-layer control. The best external cooled ducts only gave efficiencies from about 20 to 40 percent, apparently indicating a superiority for the internal arrangement. This is to be expected if consideration is taken of the fact that the external ducts suffer all the duct losses of the internal arrangement with an additional loss due to the interference effect on the rest of the wing due to its exposed position.

Most of the duct arrangements were grossly inefficient and the addition of scoops and flaps further decreased the efficiency. In further tests that are projected, a detailed study will be made in which the separate losses, such as entrance, exit, duct, core, and interference losses, will be isolated.

Effect of Pressure Drop Through Radiator

Owing to the generally low duct efficiencies of most of the arrangements tested, the useful work done in moving the air through the radiator core was a small part of the total work expended in the system. A limited number of tests (A26 to A31 inclusive) were made with screens of several meshes in front of radiator A to simulate radiators with larger pressure drops (fig. 4). The results given in table II show that the duct efficiency does not vary in a regular manner with the pressure drops and in some cases actually decreases.

Application to Design

Thus far, the quantity of air flowing through the

ducts has been given without reference to the practical requirements of an actual installation. Estimates have been made indicating that about 13,000 cubic feet of air per minute are required for the Prestone radiator to cool a 1,000-horsepower engine by means of a standard 9-inch hexagonal tube radiator having a face area of 3-1/2 square feet. An additional 4,000 cubic feet per minute are required for oil cooling using two standard Air Corps oil coolers 9 inches in diameter and 7 inches deep. Scaled to the dimensions of the model tested in the tunnel, the air-flow requirements through the Prestone duct at 100 miles per hour (as presented in table II) are about 2,500 cubic feet per minute in the climb condition and 1,300 cubic feet per minute in the high-speed condition assuming the climb to be made at 130 miles per hour and high speed at 250 miles per hour. Based on similar calculations the oil coolers would require 770 and 400 cubic feet per minute in the climb and high-speed conditions, respectively.

Reference to table II will show that air quantities commensurate with the foregoing were obtained for a number of the different arrangements with the 15-inch spanwise width of duct that was used. Obviously for any design in which the space was not limited, enlarging the duct width along the span would increase the flow, although experimental data are not available to show to what extent. Projected tests on the internal duct systems will provide this information; however, until such data are available, a satisfactory procedure may be to choose a duct combination with a high efficiency and adjust the duct width to obtain the desired flow assuming proportional increases of flow with duct width.

The power absorbed in the radiator ducts may be calculated in the following manner:

$$\text{hp.} = \frac{Q \quad \Delta P}{\eta \quad 33000} \tag{1}$$

in which

Q is the quantity of air required for cooling in cu. ft. per min.

ΔP, the pressure drop in lb. per sq. ft. across the radiator core

η, the duct efficiency as previously defined

The value of ΔP is dependent on the flight speed, degree of expansion of the duct at the radiator, and the density of the radiator core, and may be expressed as,

$$\Delta P = q \, \Delta p \left(\frac{V_R}{V}\right)^2 \qquad (2)$$

in which

q is the dynamic pressure in lb. per sq. ft. corresponding to the flight speed

Δp, the pressure drop in the radiator core in terms of the dynamic pressure at the face of the radiator

V, the free stream speed

V_R, the air speed at the radiator face

For the typical case already mentioned of a 1,000-horsepower engine in an airplane with a high speed of 250 miles per hour and a radiator core having a Δp of 4 (see fig. 4) and assuming the air speed at the radiator to be 1/4 of the free stream speed the value of ΔP is obtained by substitution in (2) as:

$$\Delta P = \frac{160 \times 4}{16} = 40 \text{ lb. per sq. ft.}$$

Using the previous estimate of 17,000 cubic feet per minute required to cool the 1,000-horsepower engine and assuming a duct efficiency of 50 percent, the horsepower required for cooling at high speed is by (1)

$$\text{hp.} = \frac{17000 \times 40}{0.5 \times 33000} = 41 \text{ hp.}$$

or 4 percent of the total horsepower. Obviously for a duct with an efficiency of 100 percent only 2 percent of the total horsepower would be utilized for cooling. This represents the minimum loss possible for the particular duct conditions that were chosen.

The possibilities of cooling with small expenditures of power by using expanding internal wing ducts of high efficiency are amply demonstrated by the foregoing calculation. These results are to be compared with expenditures of about 14 percent of the engine power as given in reference 2 for the radiators of the YO-31A airplane, and about 20 percent for external cowled radiators of a large four-engine midwing airplane. By using equations (1) and (2) and making correct substitutions of the duct constants and assumptions regarding the duct efficiency, the expected loss from the radiator duct unit may be computed for other combinations of engine horsepower and duct expansion. No consideration has been taken of the added power to carry the added weight of the larger radiators required in the expanding ducts; however, for larger airplanes in particular this factor may be shown to be relatively unimportant. For each particular design, however, it should be considered.

Langley Memorial Aeronautical Laboratory,
National Advisory Committee for Aeronautics,
Langley Field, Va., January 24, 1938.

REFERENCES

1. DeFrance, Smith J.: The N.A.C.A. Full-Scale Wind Tunnel. T.R. No. 459, N.A.C.A., 1933.

2. DeFrance, S. J.: Drag of Prestone and Oil Radiators on the YO-31A Airplane. T.N. No. 549, N.A.C.A., 1935.

TABLE Ia RADIATOR-DUCT ARRANGEMENT 'A'

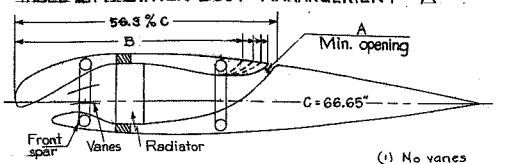

(1) No vanes

Arrangement	Radiator type	Mesh of screens	Inlet type	Outlet type	A % of C	B % of C
A1	A	—	21	36	2.75	53.0
A2	A	—	21	46	3.90	51.5
A3	A	—	23	36	2.75	53.0
A4	A	—	23	46	3.90	51.5
A5 (1)	A	—	25	36	2.75	53.0
A6 (1)	A	—	25	46	3.90	51.5
A7	A	—	33	36	2.75	53.0
A8	A	—	33	46	3.90	51.5
A9 (1)	A	—	35	36	2.75	53.0
A10 (1)	A	—	35	46	3.90	51.5
A11 (1)	A	—	43	46	3.90	51.5
A12	A	—	43	46	3.90	51.5
A13	A	—	43	36	2.75	53.0
A14	A	—	45	36	2.75	53.0
A15	A	—	45	46	3.90	51.5
A16	A	—	55	26	1.60	54.7
A17	A	—	55	36	2.75	53.0
A18	A	—	55	46	3.90	51.5
A19	A	—	55	56	5.48	49.1
A20	A	—	63	36	2.75	53.0
A21	A	—	63	46	3.90	51.5
A22	A	—	63	56	5.48	49.1
A23	A	—	43	56	5.48	49.1
A24	A	—	45	56	5.48	49.1
A25	A	—	66	56	5.48	49.1
A26	A	16	43	56	5.48	49.1
A27	A	40	43	56	5.48	49.1
A28	A	16	55	56	5.48	49.1
A29	A	40	55	56	5.48	49.1
A30	A	16	63	56	5.48	49.1
A31	A	40	63	56	5.48	49.1

TABLE Ib RADIATOR-DUCT ARRANGEMENT 'B'

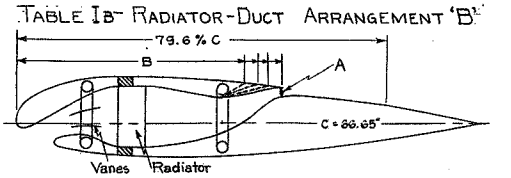

Arrangement	Radiator type	Inlet type	Outlet type	A % of C	B % of C
B1	A	45	47	3.90	52.1
B2	A	45	57	5.48	49.1
B3	A	55	27	1.60	57.0
B4	A	55	37	2.75	54.2
B5	A	55	47	3.90	52.1
B6	A	55	57	5.48	49.1

TABLE Ic RADIATOR-DUCT ARRANGEMENT 'C'

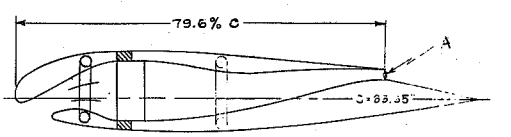

Arrangement	Radiator type	Inlet type	Outlet type	A % of C	B % of C
C1	A	45	28	2.10	79.6
C2	A	55	28	2.10	79.6

TABLE Id RADIATOR-DUCT ARRANGEMENT 'D'

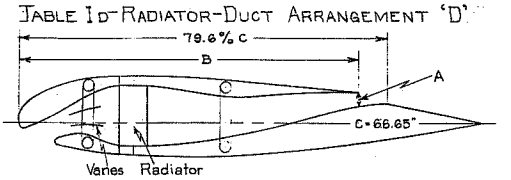

Arrangement	Radiator type	Inlet type	Outlet type	A % of C	B % of C
D1	A	45	38	2.28	73.3
D2	A	55	38	2.28	73.3

TABLE Ie RADIATOR-DUCT ARRANGEMENT 'E'

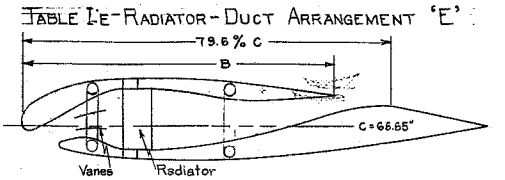

Arrangement	Radiator type	Inlet type	Outlet type	A % of C	B % of C
E1	A	45	48	2.78	67.0
E2	A	55	48	2.78	67.0

TABLE If RADIATOR-DUCT ARRANGEMENT 'F'

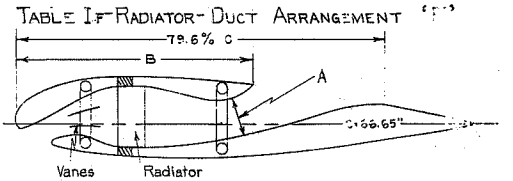

Arrangement	Radiator type	Inlet type	Outlet type	A % of C	B % of C
F1	A	55	78	7.88	51.5
F2	A	66	78	7.88	51.5

TABLE Ig RADIATOR-DUCT ARRANGEMENT 'G'

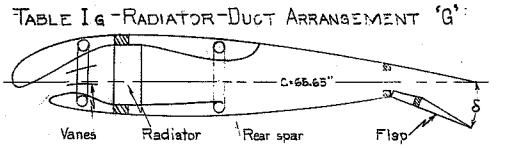

Arrangement	Radiator type	Inlet type	Exit flap angle, δ
G1	A	43	5°
G2	A	43	10
G3	A	43	15
G4	A	43	20
G5	A	43	25
G6	A	55	5
G7	A	55	10
G8	A	55	15
G9	A	55	20
G10	A	55	25
G11	A	63	5
G12	A	63	15
G13	A	63	25

TABLE I-H - RADIATOR-DUCT ARRANGEMENT 'H'

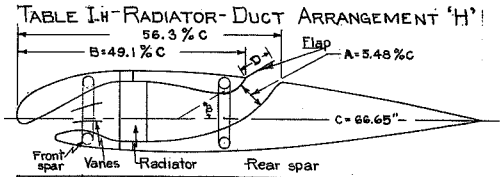

Arrangement	Radiator type	Inlet type	Outlet type	Flap style	Flap length, D	Flap angle, θ
H1	A	45	56	A	4 in.	45°
H2	A	66	56	A	4	45
H3	A	66	56	A	4	30
H4	A	45	56	B	6	15
H5	A	55	56	B	6	15
H6	A	66	56	B	6	15
H7	A	45	56	B	6	30
H8	A	55	56	B	6	30
H9	A	45	56	B	6	15
H10	A	55	56	B	6	15

TABLE I-I - RADIATOR-DUCT ARRANGEMENT 'I'

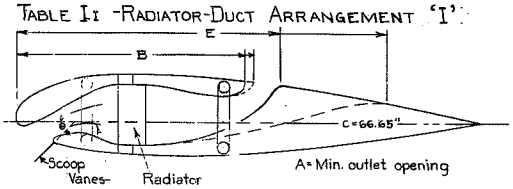

Arrangement	Radiator type	Inlet type	Scoop angle, θ	Outlet type	A % of C	B % of C	E % of C
I1	A	66	45°	56	5.48	49.1	56.3
I2	A	66	30	56	5.48	49.1	56.3
I3	A	66	30	78	7.88	51.5	79.6

TABLE I-J - RADIATOR-DUCT ARRANGEMENT 'J'

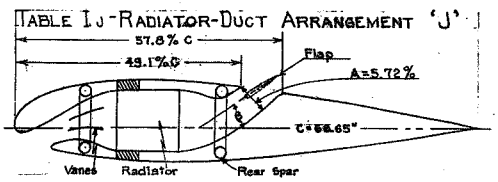

Arrangement	Radiator type	Inlet type	Exit flap angle δ
J1	B	55	Flap off
J2	B	55	33°

TABLE I-K - RADIATOR-DUCT ARRANGEMENT 'K'

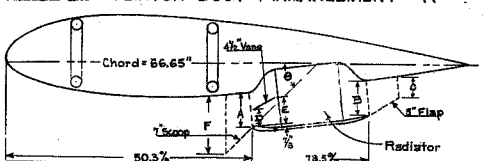

Arrangement	Radiator type	Radiator A	Radiator B	Flap C	Vane D	Vane E	Scoop F	Scoop θ
K1	B	5 in.	5 in.	—	—	—	—	—
K2	B	5	5	3⅜ in.	—	—	—	—
K3	B	4½	4½	—	2 in.	3⅜ in.	—	—
K4	B	4½	4½	3⅜	—	—	—	—
K5	B	4	4	—	2⅛	3⅜	—	—
K6	B	4	4	2	2⅛	3⅜	—	—
K7	B	3	3	—	—	—	—	—
K8	B	3	3	—	—	—	3½ in.	30°
K9	B	3	3	—	—	—	8	45°

TABLE I-L - RADIATOR-DUCT ARRANGEMENT 'L'

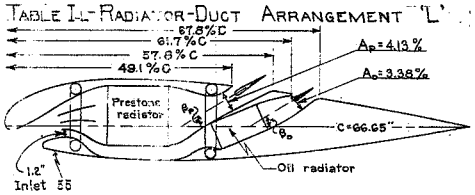

Arrangement	Radiator type	Prestone flap θ_p, degrees	Oil flap θ_o, degrees
L1	B	0	0
L2	B	33	33
L3	B	Off	Off
L4 (1)	B	Off	Off

(1) Two upper vanes out.

TABLE I-N - RADIATOR-DUCT ARRANGEMENT 'N'

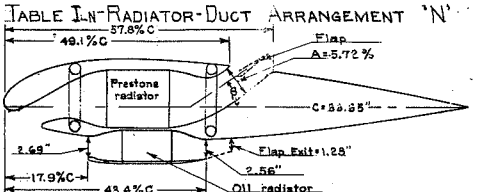

Arrangement	Radiator type	Prestone Inlet type	Prestone Flap	Prestone θ	Oil Flap
N1	B	55	Off	—	Off
N2	B	55	On	13°	Off
N3	B	55	On	33°	Off
N4	B	55	Off	—	On

TABLE I-M - RADIATOR-DUCT ARRANGEMENT 'M'

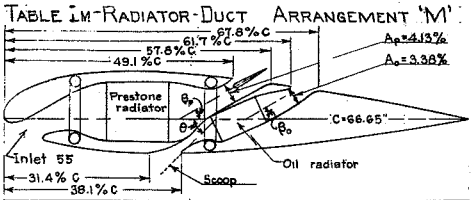

Arrangement	Radiator type	Prestone flap, θ_p, degrees	Oil flap, θ_o, degrees	Oil scoop, θ, degrees
M1	B	Off	Off	Off
M2	B	33	Off	Off
M3	B	Off	Off	30
M4	B	Off	Off	45
M5	B	33	Off	45

TABLE I-P - RADIATOR-DUCT ARRANGEMENT 'P'

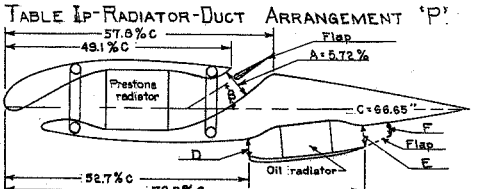

Arrangement	Radiator type	Prestone Inlet	Prestone Flap	Prestone θ	Oil D	Oil E	Oil F
P1	B	55	Off	—	2.69"	2.56"	—
P2	B	55	On	13°	2.69	2.56	—
P3	B	55	On	33°	2.69	2.56	—
P4	B	55	Off	—	2.69	2.56	1.44"
P5	B	55	Off	—	2.19"	2.06"	—

TABLE IIA - AERODYNAMIC CHARACTERISTICS OF DUCTS

Typical diagrams	Arrangement	Test vel., m.p.h.	ΔC_D, % C_L=0.15	ΔC_D, % C_L=0.70	$\Delta C_{L\,max.}$	Air quantity per radiator cu.ft. per min. at 100 m.p.h. C_L=0.15	Air quantity per radiator cu.ft. per min. at 100 m.p.h. C_L=0.70	Duct efficiency % C_L=0.15
	A1	60	6.2	0.8	0.04	1430	1920	14.8
	A2	60	6.9	-2.5	0.04	1000	1450	4.6
		100	6.9	-1.3	—	770	1,350	2.0
	A3	60	4.8	1.0	-0.02	1060	730	7.8
		100	6.3	4.5	—	1,430	880	14.6
	A4	60	5.5	-6.1	0.02	770	930	2.6
	A5	60	6.2	1.8	0.02	780	1,550	2.4
		100	4.9	-2.4	—	150	1,520	0.02
	A6	60	4.8	-2.3	0.04	850	1,680	4.0
		100	6.3	0.3	—	560	1,660	0.8
	A7	60	9.6	1.8	0.08	1,580	2,150	12.8
	A8	60	11.7	-0.5	0.08	1,680	1,850	12.6
	A9	60	6.9	0.3	0.06	680	2,590	1.4
	A10	60	2.8	-2.8	0.06	2,200	2,800	100+
	A11	60	9.6	-4.6	0.02	1,660	2,570	14.8
	A12	60	10.3	-0.3	0.08	1,700	2,830	14.8
		100	9.0	-1.3	—	1,920	2,750	24.6
	A13	60	8.9	0	0.12	1,300	2,370	7.6
		100	8.4	-0.8	—	1,300	2,300	8.2
	A14	60	-0.7	0	0.06	1,080	2,750	100+
	A15	60	2.1	-1.3	0.06	1,520	2,920	50.4
	A16	60	6.2	2.5	0.08	1,750	2,350	26.8
	A17	60	8.9	-0.5	0.10	2,000	2,950	28.0
		100	5.5	-1.3	—	2,570	2,850	96.8

TABLE IIB - AERODYNAMIC CHARACTERISTICS OF DUCTS (CONT.)

Typical diagrams	Arrangement	Test vel., m.p.h.	ΔC_D, % C_L=0.15	ΔC_D, % C_L=0.70	$\Delta C_{L\,max.}$	Air quantity per radiator cu.ft. per min. at 100 m.p.h. C_L=0.15	Air quantity per radiator cu.ft. per min. at 100 m.p.h. C_L=0.70	Duct efficiency % C_L=0.15
	A18	60	11.6	-1.3	0.10	2,210	3,350	28.8
		100	8.3	1.9	—	2,360	3,390	49.6
	A19	60	11.0	-1.0	0.06	2,600	3,800	49.6
	A20	60	8.2	1.8	0.04	2,140	2,230	37.2
		100	4.9	-0.3	—	2,250	2,300	73.0
	A21	60	5.5	-1.3	0	3,200	2,880	100+
		100	5.6	1.3	—	2,400	2,800	77.6
	A22	60	8.9	-1.3	-0.02	2,420	2,780	49.4
	A23	100	11.1		—	2,170	2,470	28.8
	A24	60	4.8	-1.3	0.02	910	2,250	4.8
	A25	60	—	—	—	—	2,890	—
	A26	60	13.8	-2.3	0.04	2,260	2,630	38.4
	A27	60	15.8	-0.5	0.04	1,810	2,180	22.8
	A28	60	16.5	-4.1	0.04	2,250	3,060	26.6
	A29	60	15.1	-2.0	0.04	1,910	2,950	28.0
	A30	60	16.5	-0.3	0.04	2,480	3,100	35.6
	A31	60	15.6	-0.8	0.02	2,410	2,500	53.8
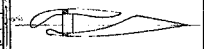	B1	60	5.5	-3.1	—	860	2,540	3.6
	B2	60	9.6	-2.0	—	1,080	2,480	4.0
	B3	60	8.2	2.0	—	1,670	1,820	17.6
	B4	60	11.0	-3.6	—	2,060	2,880	24.6
	B5	60	13.1	-3.8	—	2,430	3,020	34.2
	B6	60	16.5	-2.0	—	2,230	3,140	20.8

TABLE IIC - AERODYNAMIC CHARACTERISTICS OF DUCTS (CONT.)

Typical diagrams	Arrangement	Test vel., m.p.h.	ΔC_D, % C_L=0.15	ΔC_D, % C_L=0.70	$\Delta C_{L\,max.}$	Air quantity per radiator cu.ft. per min. at 100 m.p.h. C_L=0.15	Air quantity per radiator cu.ft. per min. at 100 m.p.h. C_L=0.70	Duct efficiency % C_L=0.15
	C1	60	6.9	2.5	—	1,410	2,580	12.6
	C2	60	7.6	-1.3	—	2,060	2,060	36.0
	D1	60	5.5	2.8	—	495	2,060	0.6
	D2	60	5.5	2.3	—	1,780	2,060	32.0
	E1	60	3.4	2.0	—	1,275	2,370	19.0
	E2	60	12.4	5.5	—	1,820	2,450	15.2
	F1	60	15.8	-2.3	0.04	2,350	3,040	25.6
	F2	60	—	—	—	—	3,510	—
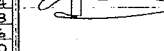	G1	60	17.8	1.3	0.12	1,900	2,430	12.0
	G2	60	19.2	0.8	0.12	1,820	2,520	9.8
	G3	60	28.9	3.8	0.22	1,950	3,050	8.0
	G4	60	35.0	-0.5	0.28	1,900	3,350	6.2
	G5	60	49.4	4.3	0.34	2,530	3,350	10.2
	G6	60	8.2	3.8	0.10	1,300	2,950	8.4
	G7	60	16.5	6.1	0.16	1,950	2,950	14.0
	G8	60	23.4	-1.8	0.18	2,150	3,170	13.2
	G9	60	37.0	1.8	0.20	2,800	3,250	18.4
	G10	60	48.8	8.1	0.32	3,250	3,520	22.0
	G11	60	4.8	4.3	0.10	2,100	2,220	80.0
	G12	60	24.8	1.3	0.08	2,270	2,500	14.6
	G13	60	53.0	5.6	0.22	2,050	2,760	5.0

TABLE IID - AERODYNAMIC CHARACTERISTICS OF DUCTS (CONT.)

Typical diagrams	Arrangement	Test vel., m.p.h.	ΔC_D, % C_L=0.15	ΔC_D, % C_L=0.70	$\Delta C_{L\,max.}$	Air quantity per radiator cu.ft. per min. at 100 m.p.h. C_L=0.15	Air quantity per radiator cu.ft. per min. at 100 m.p.h. C_L=0.70	Duct efficiency % C_L=0.15
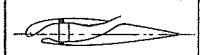	H1	60	—	—	—	—	2,760	—
	H2	60	—	—	—	—	3,590	—
	H3	60	—	—	—	—	3,470	—
	H4	60	—	—	—	—	2,690	—
	H5	60	—	—	—	—	2,980	—
	H6	60	—	—	—	—	2,980	—
	H7	60	—	—	—	—	2,890	—
	H8	60	—	—	—	—	2,880	—
	H9	60	—	—	—	—	2,860	—
	H10	60	—	—	—	—	2,960	—
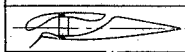	I1	60	—	—	—	—	2,860	—
	I2	60	—	—	—	—	2,970	—
	I3	60	—	—	—	—	3,760	—
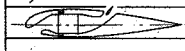	J1	60	10.0	6.2	-0.02	790	2,510	1.4
	J2	60	25.3	16.8	0	1,070	2,570	1.4
	K1	60	15.3	5.4	0	2,860	2,920	44.4
	K2	60	17.3	3.8	0.02	2,040	2,110	14.2
	K3	60	14.7	3.2	-0.04	2,060	2,210	17.4
	K4	60	13.3	-1.9	-0.02	1,570	1,730	8.4
	K5	60	16.0	4.8	0	1,630	1,810	7.8
		100	12.0	2.7	—	2,020	2,020	20.4
	K6	60	9.3	-0.5	0	960	470	2.8
	K7	60	8.6	-1.0	-0.02	1,800	2,180	19.8
	K8	60	64.0	8.1	-0.06	2,440	2,380	6.6
	K9	60	85.0	16.1	-0.04	2,580	2,590	5.8

TABLE IIE - AERODYNAMIC CHARACTERISTICS OF DUCTS (CONT.)

Typical diagrams	Arrangement	Test vel., m.p.h.	ΔC_D, % C_L=0.15	ΔC_D, % C_L=0.70	$\Delta C_{L\,max.}$	Air quantity per radiator cu.ft. per min. at 100 m.p.h. Prestone radiator C_L=0.15	Prestone radiator C_L=0.70	Oil radiator C_L=0.15	Oil radiator C_L=0.70	Duct efficiency % C_L=0.15
	L1	60	2.0	4.3	0.08	—	—	—	—	—
	L2	60	26.6	16.2	-0.18	430	1,690	320	420	0.6
	L3	60	16.7	16.2	0.04	460	1,590	360	410	1.2
		100	10.0	7.0	—	610	1,660	350	320	2.2
	L4	60	17.3	12.4	0.06	530	1,740	370	410	1.4
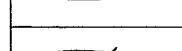	M1	60	15.3	19.5	0	620	1,790	120	500	0.4
		100	11.9	19.5	—	735	1,730	120	550	1.0
	M2	60	28.6	22.0	0.04	350	1,740	190	550	0.2
	M3	60	23.4	15.7	0.06	555	1,570	430	520	1.4
	M4	60	30.7	15.0	0.04	690	1,720	500	510	1.8
	M5	60	43.0	25.7	0.04	660	1,930	520	560	1.4
	N1	60	20.0	8.9	-0.02	1,030	2,440	1,430	1,355	54.6
		100	17.3	4.0	—	1,700	2,620	1,480	1,440	76.8
	N2	60	17.3	8.7	0.02	990	1,860	1,510	1,422	73.8
	N3	60	33.4	10.0	-0.04	810	2,590	1,420	1,390	31.6
	N4	60	22.6	10.0	0	870	2,380	850	970	10.6
	P1	60	20.0	6.8	-0.20	740	2,500	1,030	1,280	20.4
		100	15.2	8.1	—	1,370	2,460	1,120	1,275	58.8
	P2	60	18.7	8.1	-0.28	760	2,060	1,030	1,230	21.8
	P3	60	33.5	10.8	0	810	2,580	1,240	1,300	21.0
	P4	60	20.0	-1.4	-0.06	840	2,240	600	820	4.4
	P5	60	18.7	4.0	-0.06	950	2,400	880	1,110	16.2

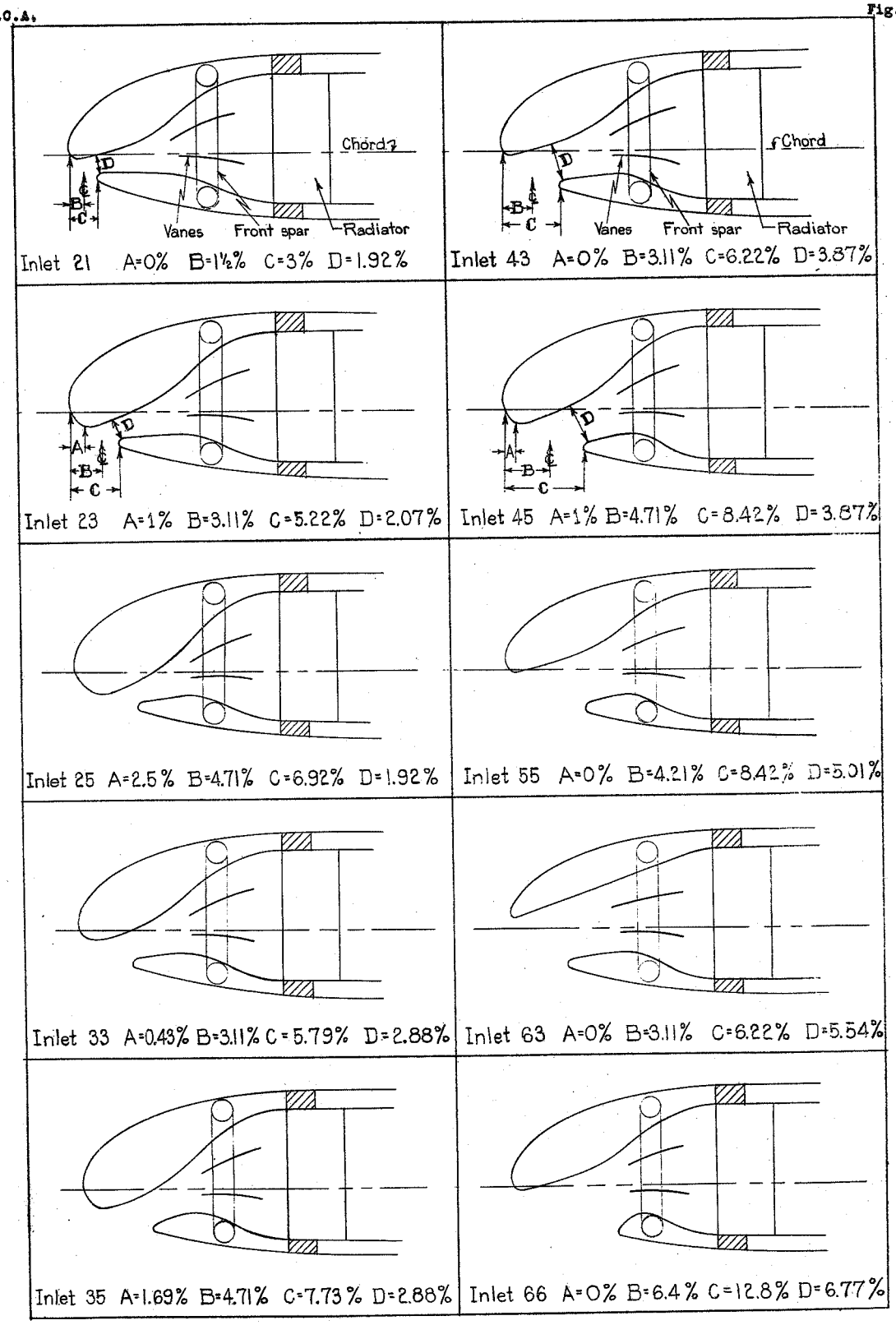

RADIATOR INLET TYPES

Figure 1. All percentages based on 66.65 in. chord

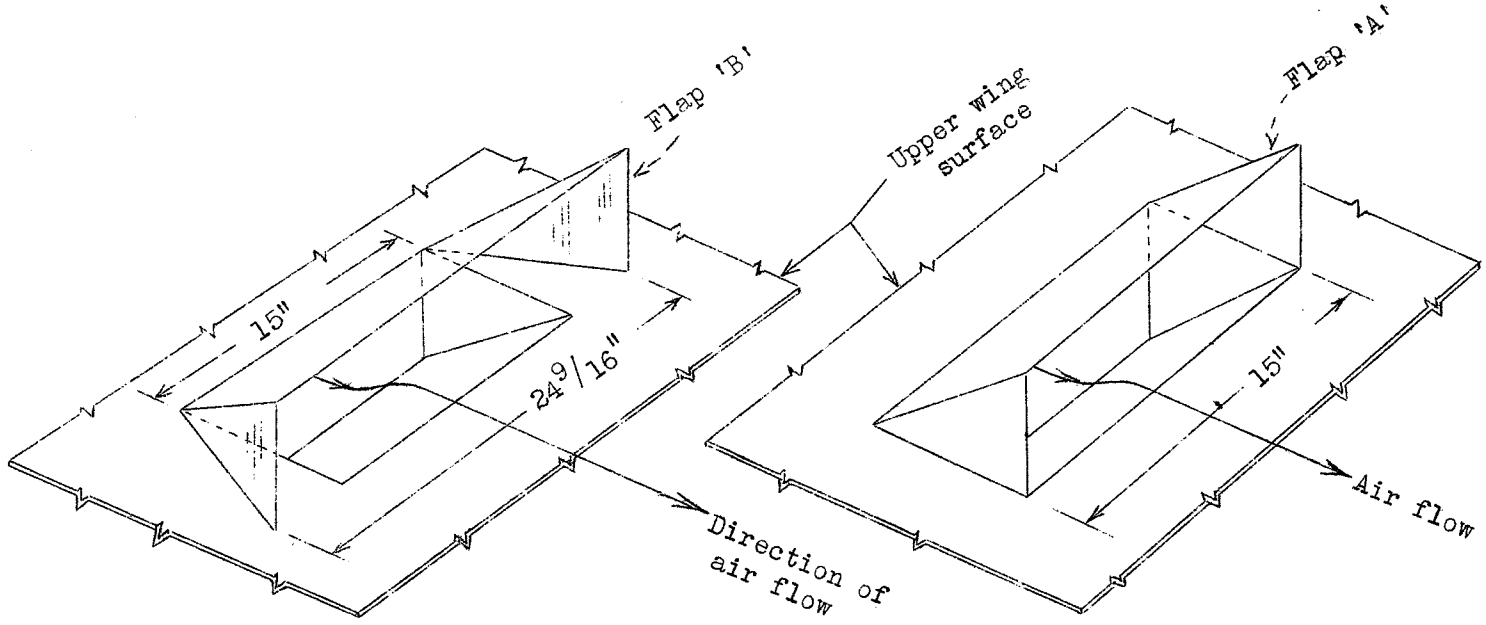

Figure 2. - Radiator-duct flap styles

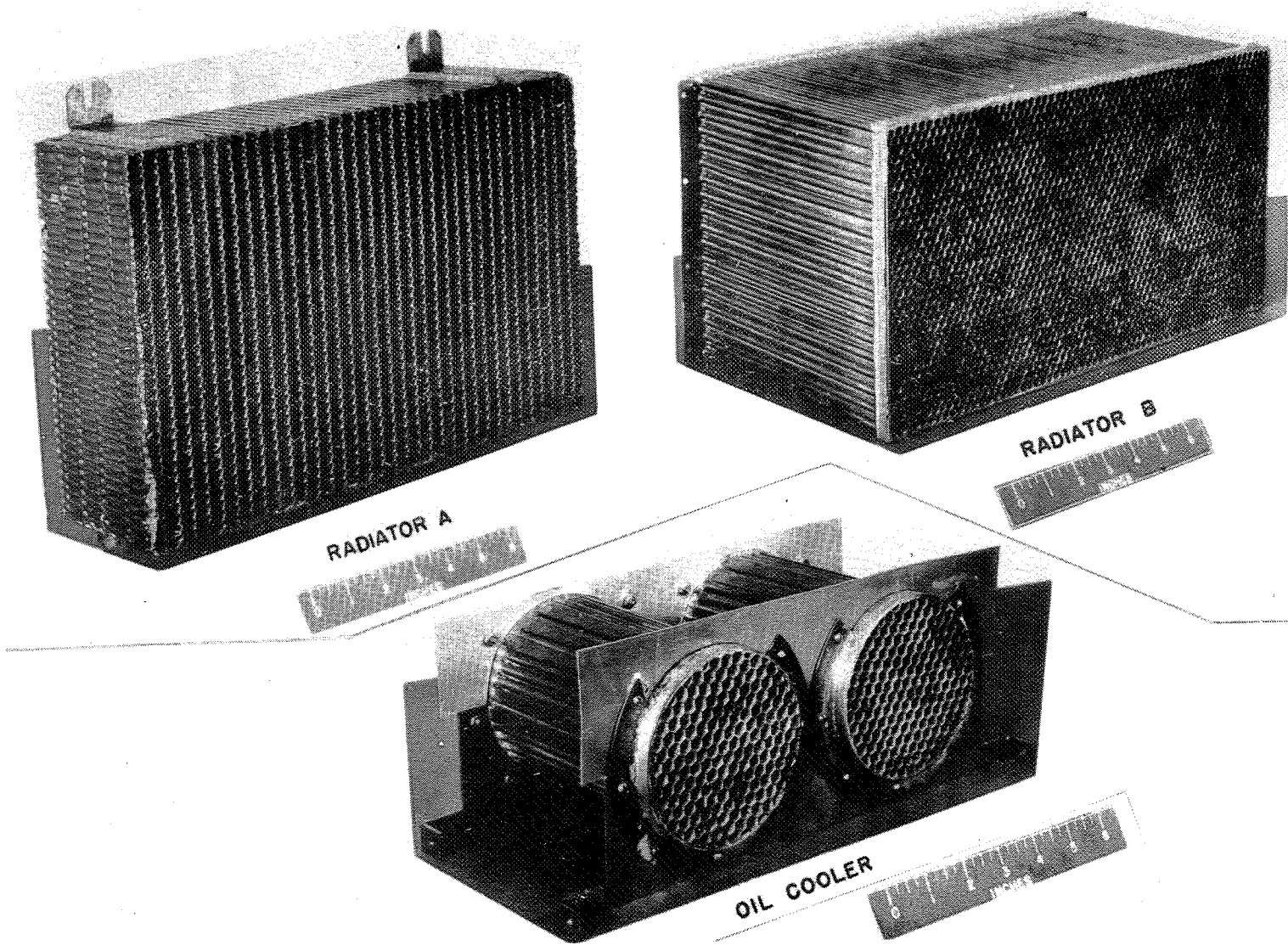

Figure 3.- Photograph of Prestone and oil radiators that were tested in the ducts.

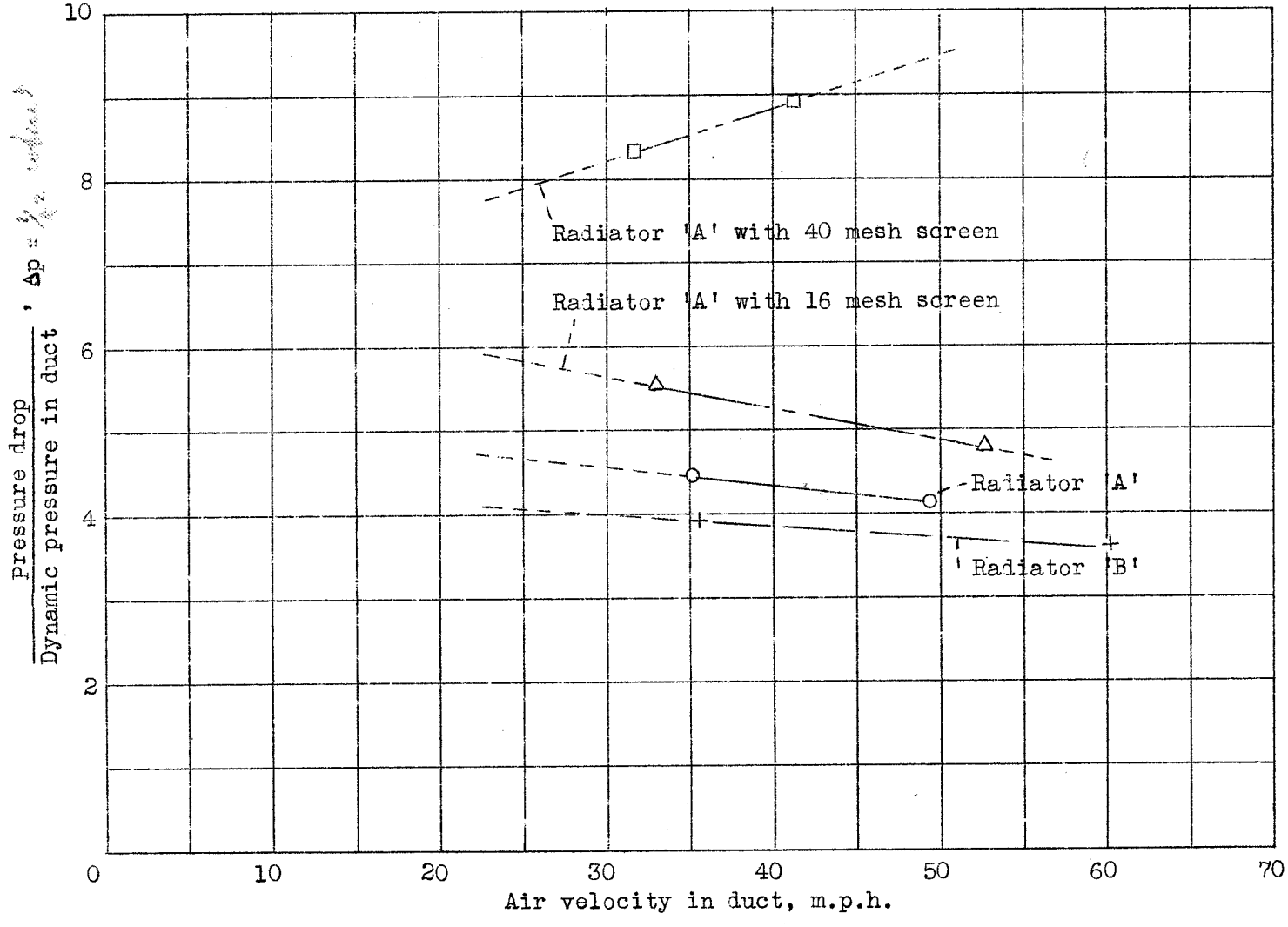

Figure 4.- Pressure drops of the various radiators used.

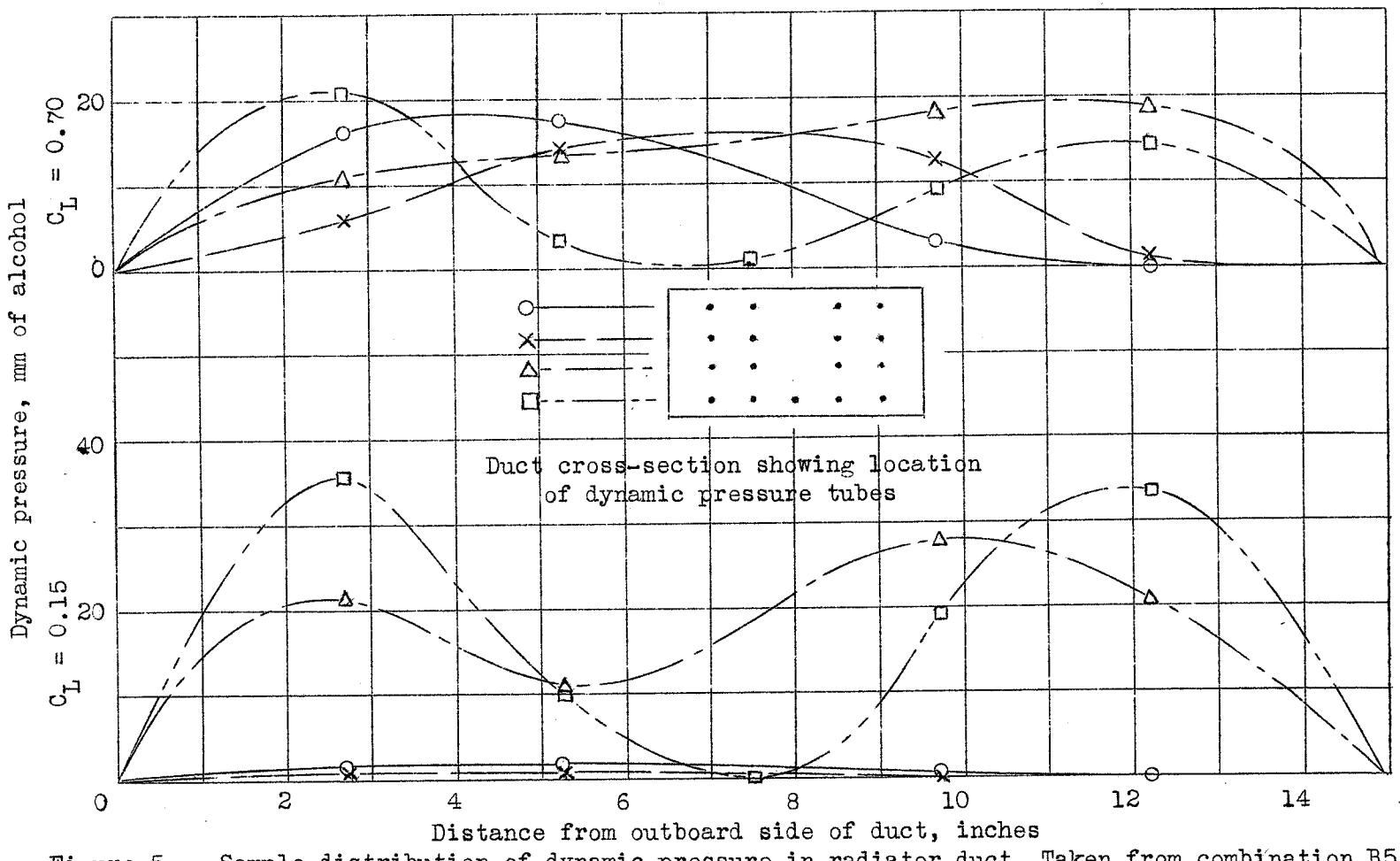

Figure 5. - Sample distribution of dynamic pressure in radiator duct. Taken from combination B5

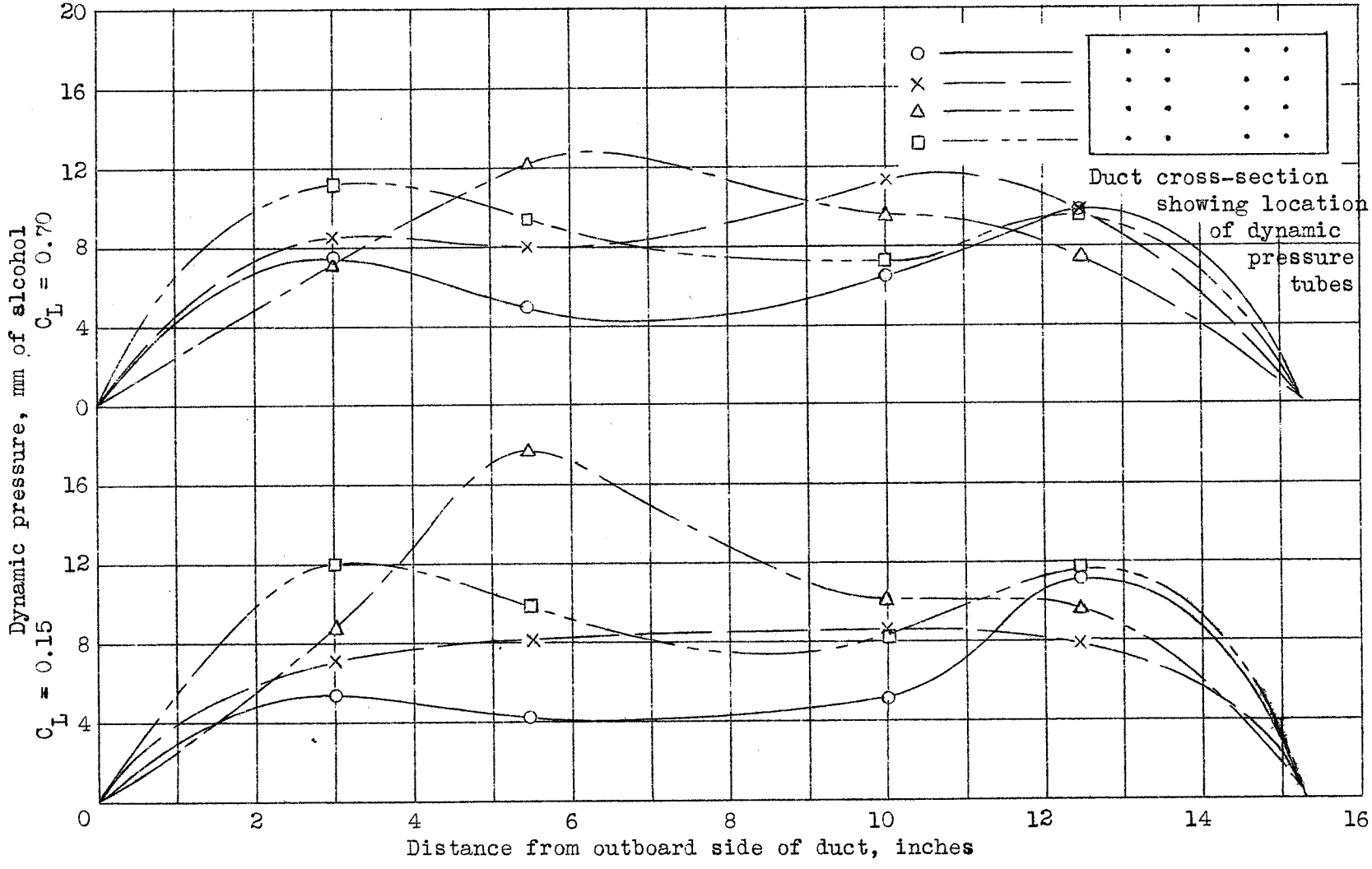

Figure 6. - Sample distribution of dynamic pressure in radiator duct. Taken from combination K1.

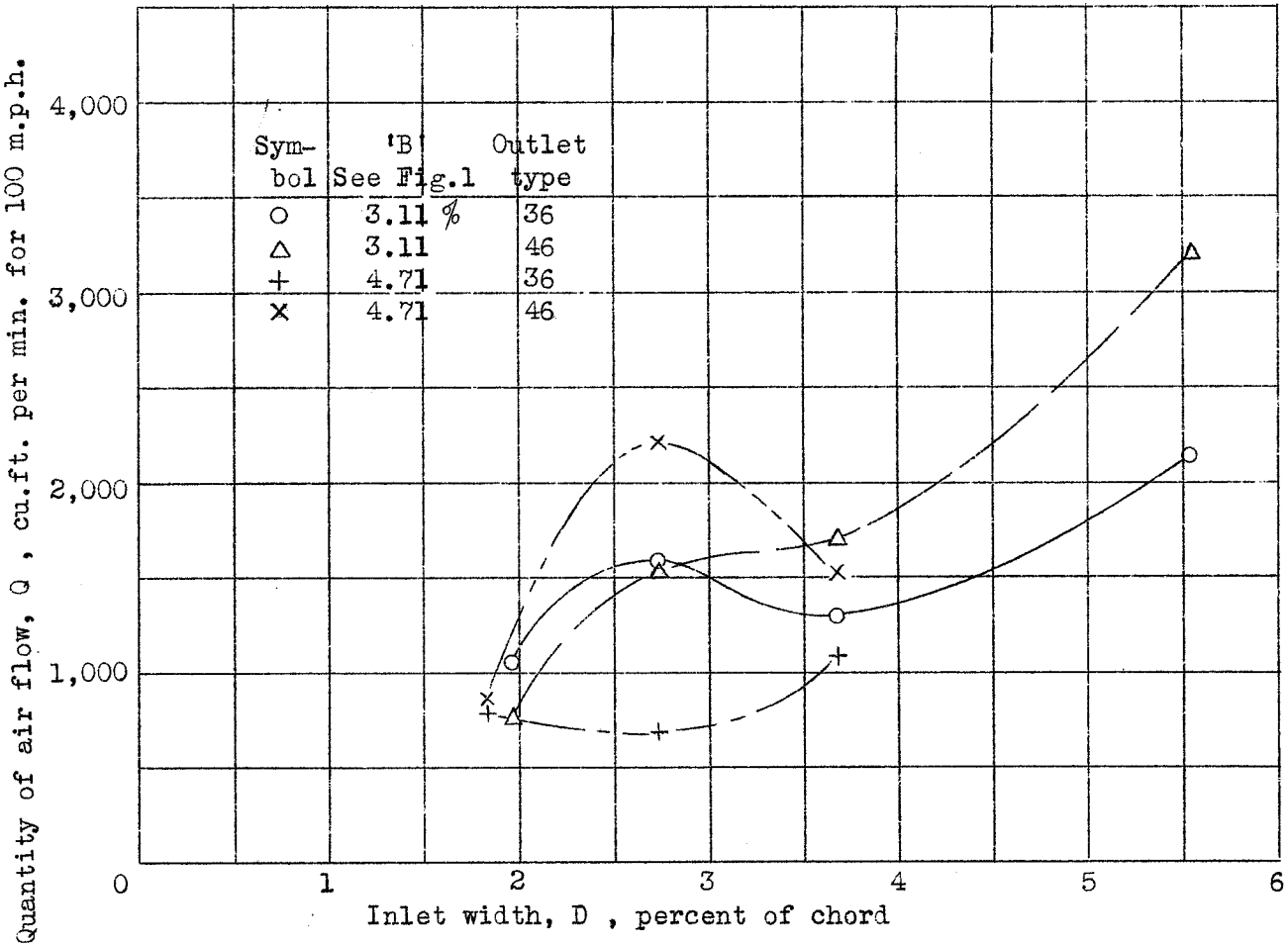

Figure 7. - Variation in air flow with inlet width. Test velocity = 60 m.p.h.
Lift coefficient = 0.15

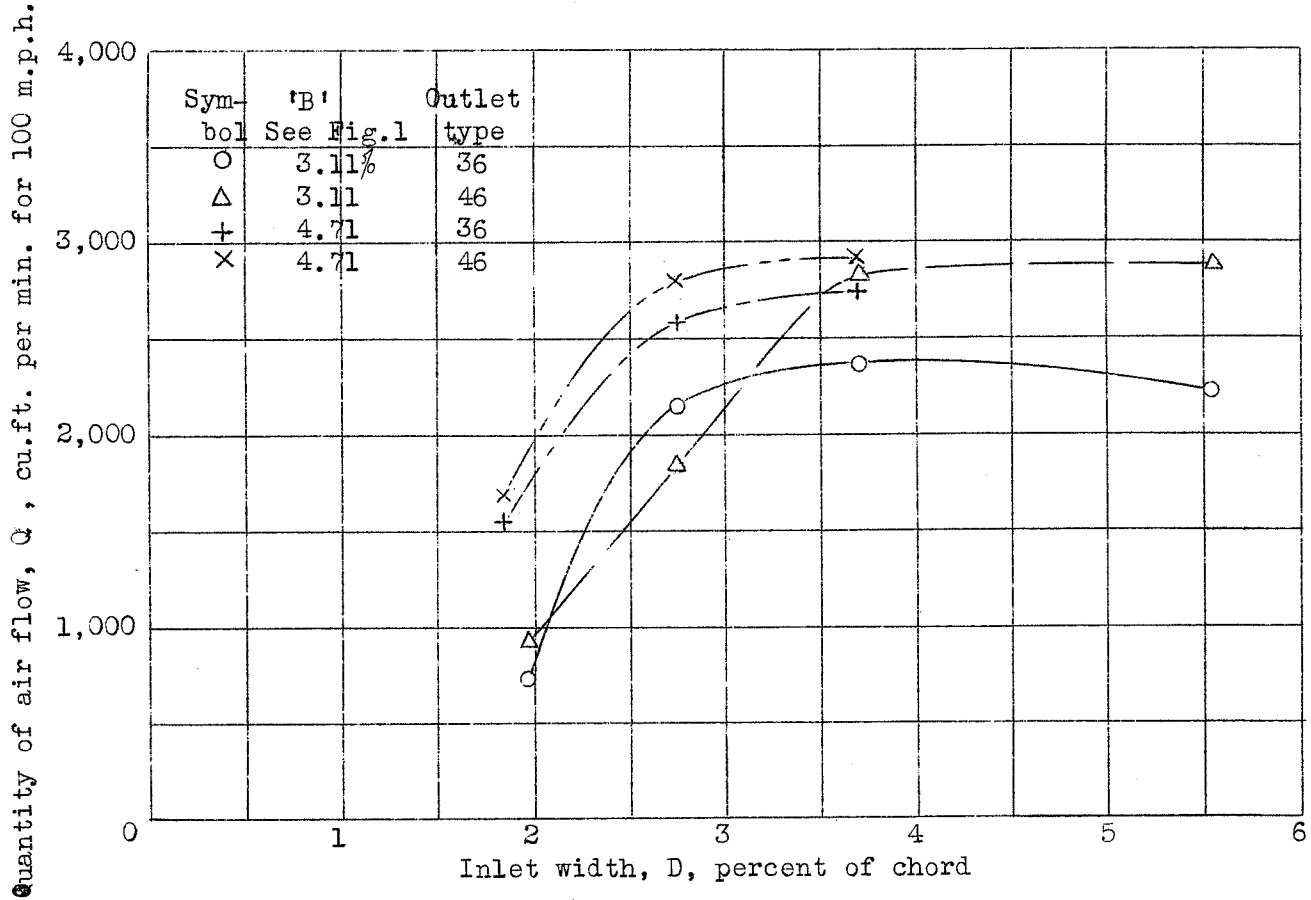

Figure 8. - Variation in air flow with inlet width. Test velocity = 60 m.p.h.
Lift coefficient = 0.70

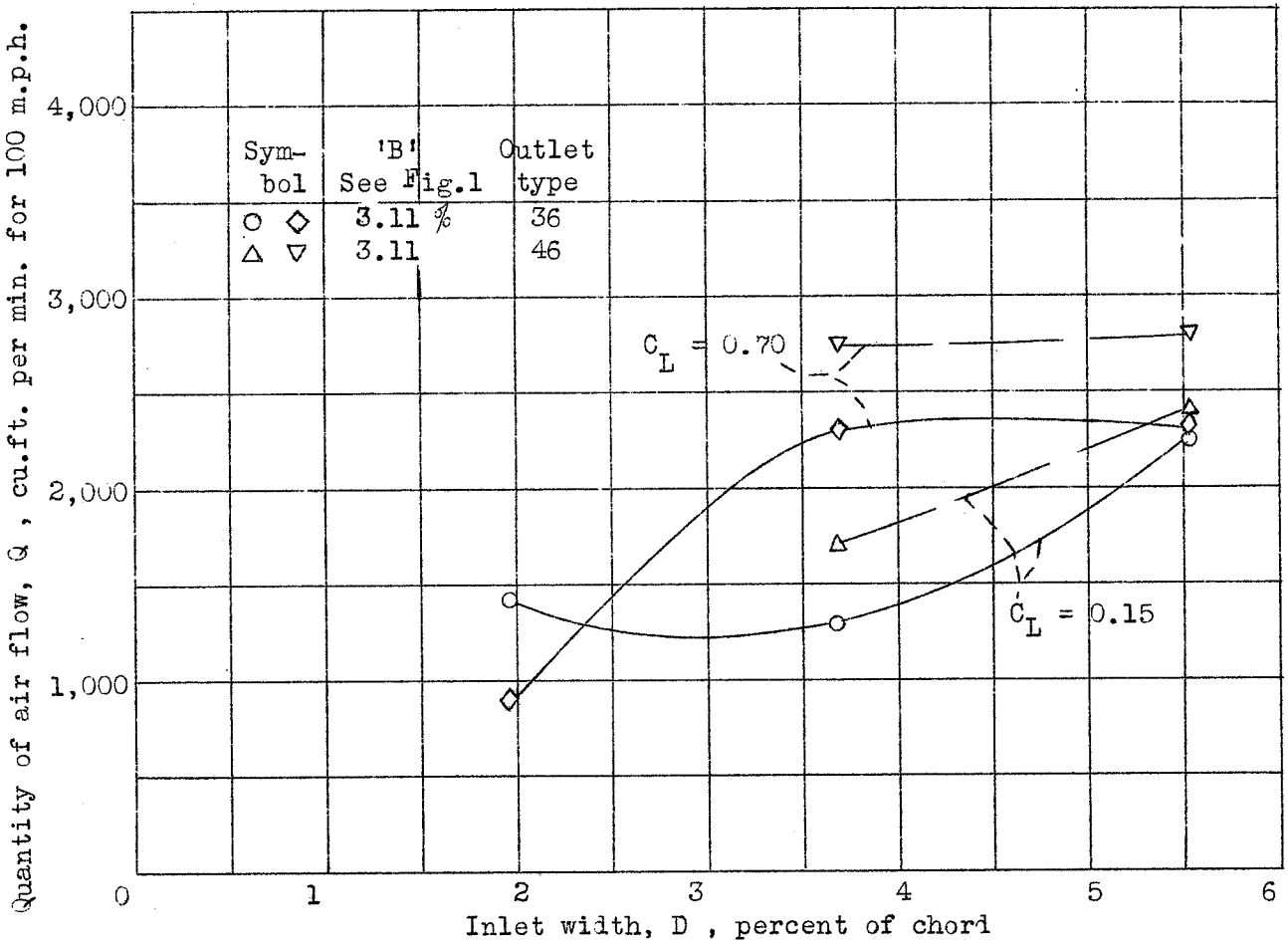

Figure 9. - Variation in air flow with inlet width. Test velocity = 100 m.p.h.

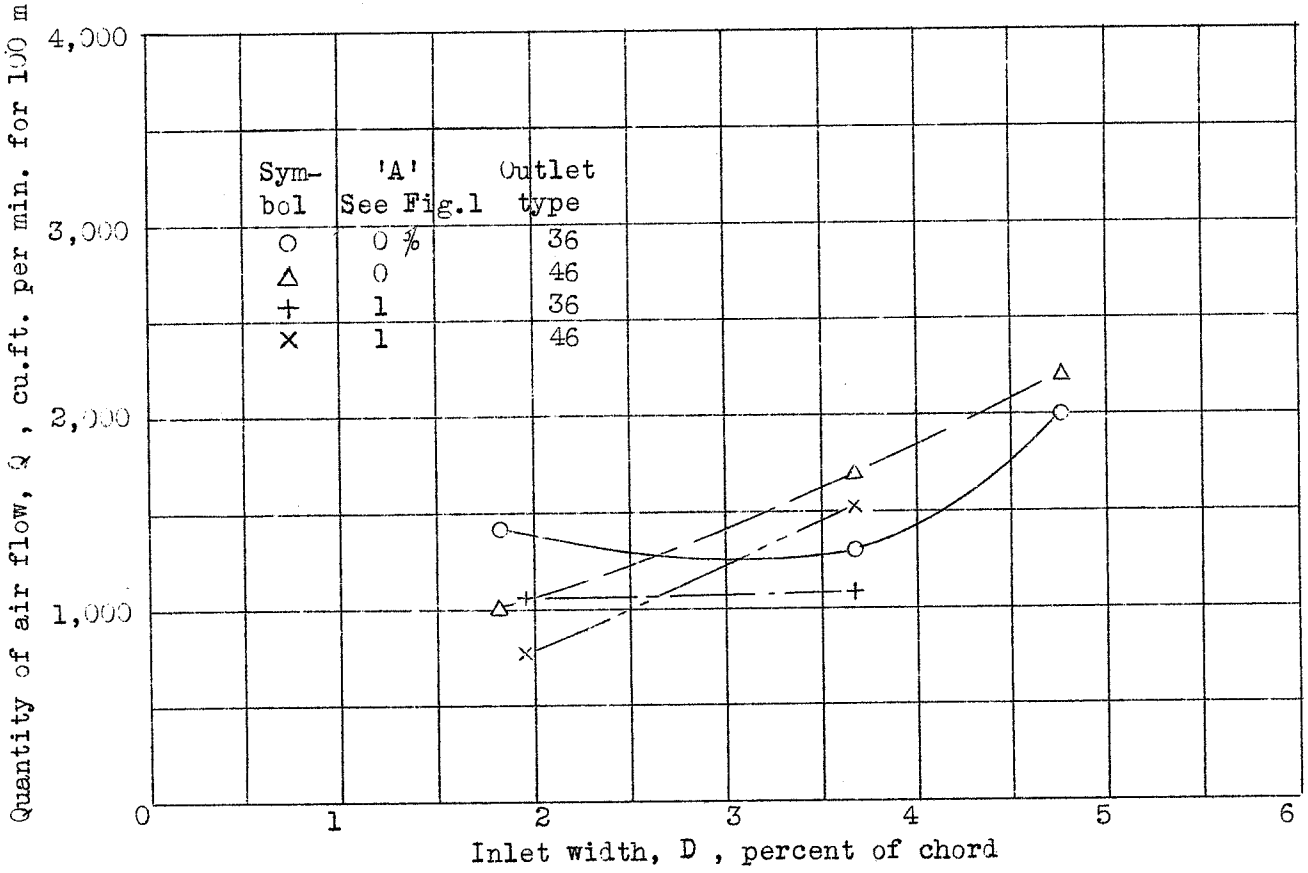

Figure 10. - Variation in air flow with inlet width. Test velocity = 60 m.p.h. Lift coefficient = 0.15

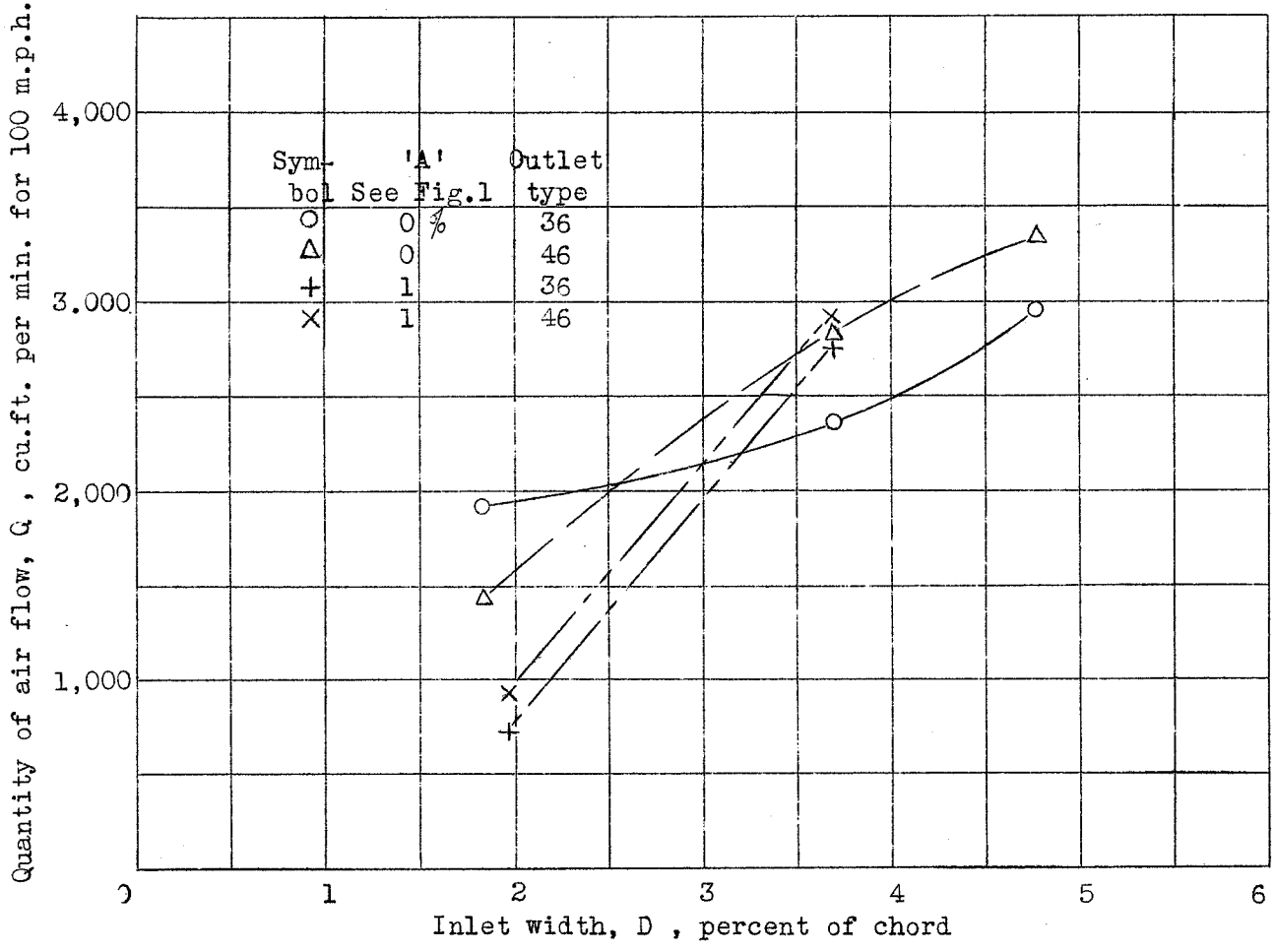

Figure 11. - Variation in air flow with inlet width. Test velocity = 60 m.p.h. Lift coefficient = 0.70

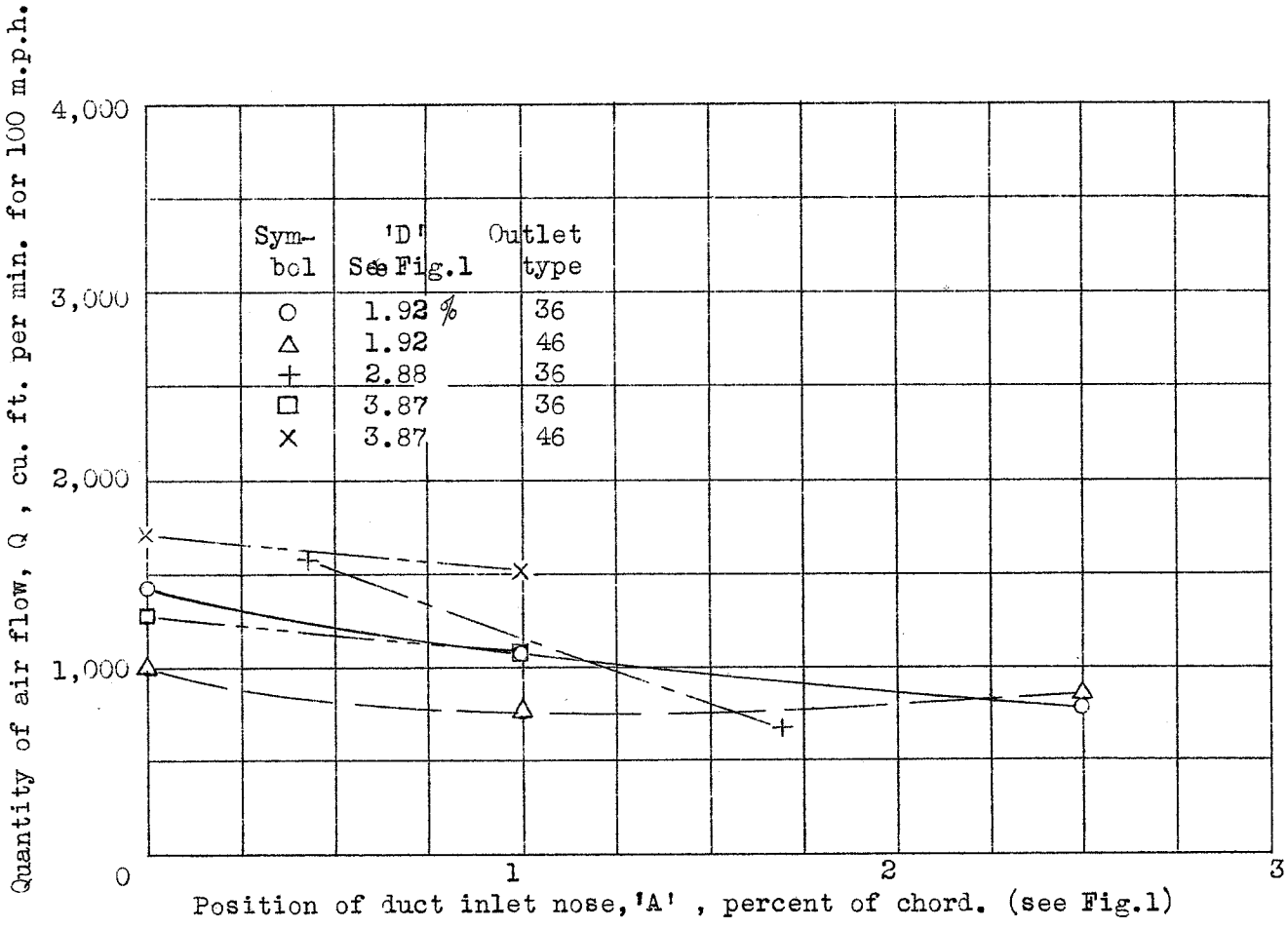

Figure 12. – Variation in air flow with the position of the duct inlet nose. Test velocity = 60 m.p.h. Lift coefficient = 0.15

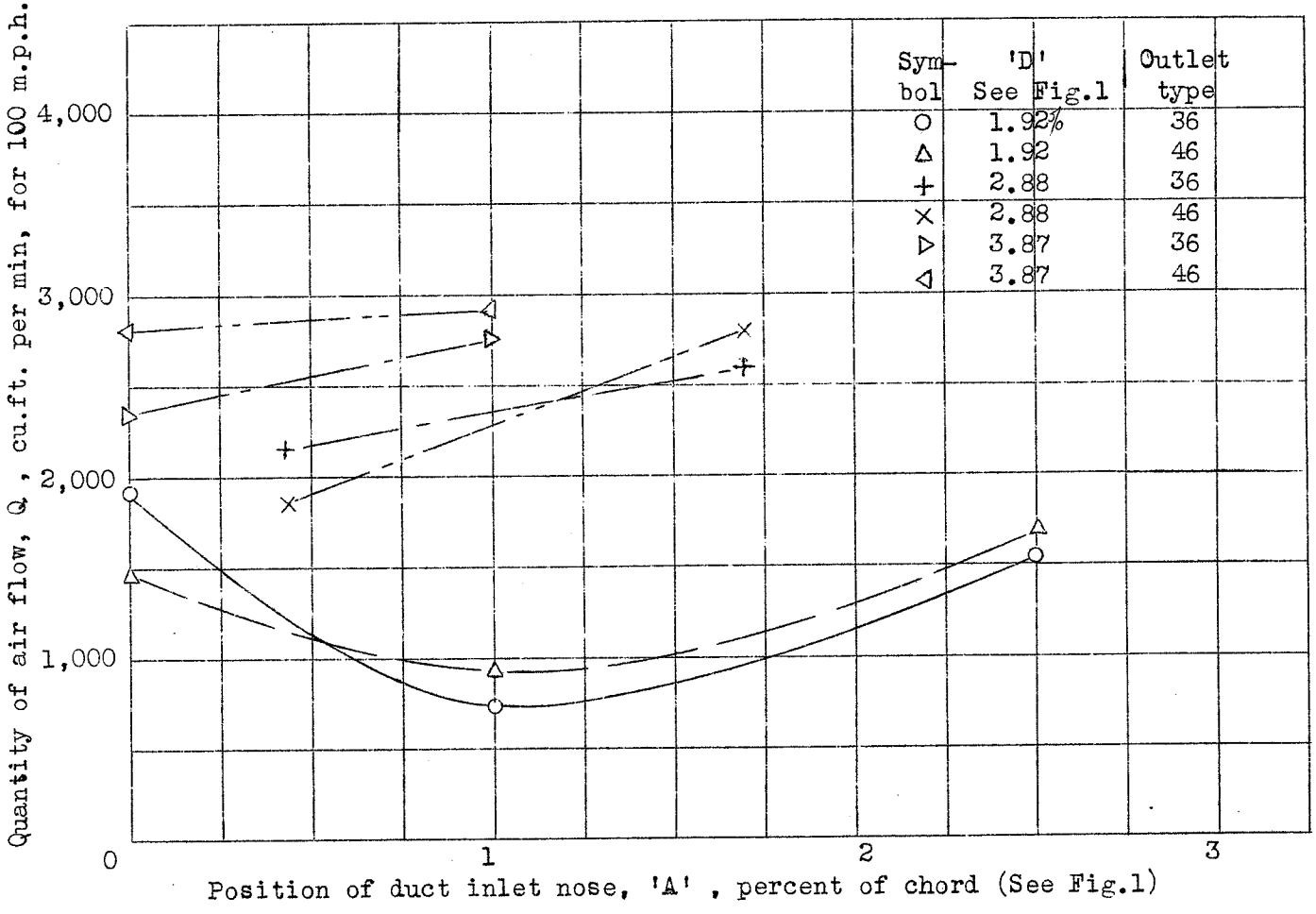

Figure 13. - Variation in air flow with the position of the duct inlet nose. Test velocity = 60 m.p.h. Lift coefficient = 0.70

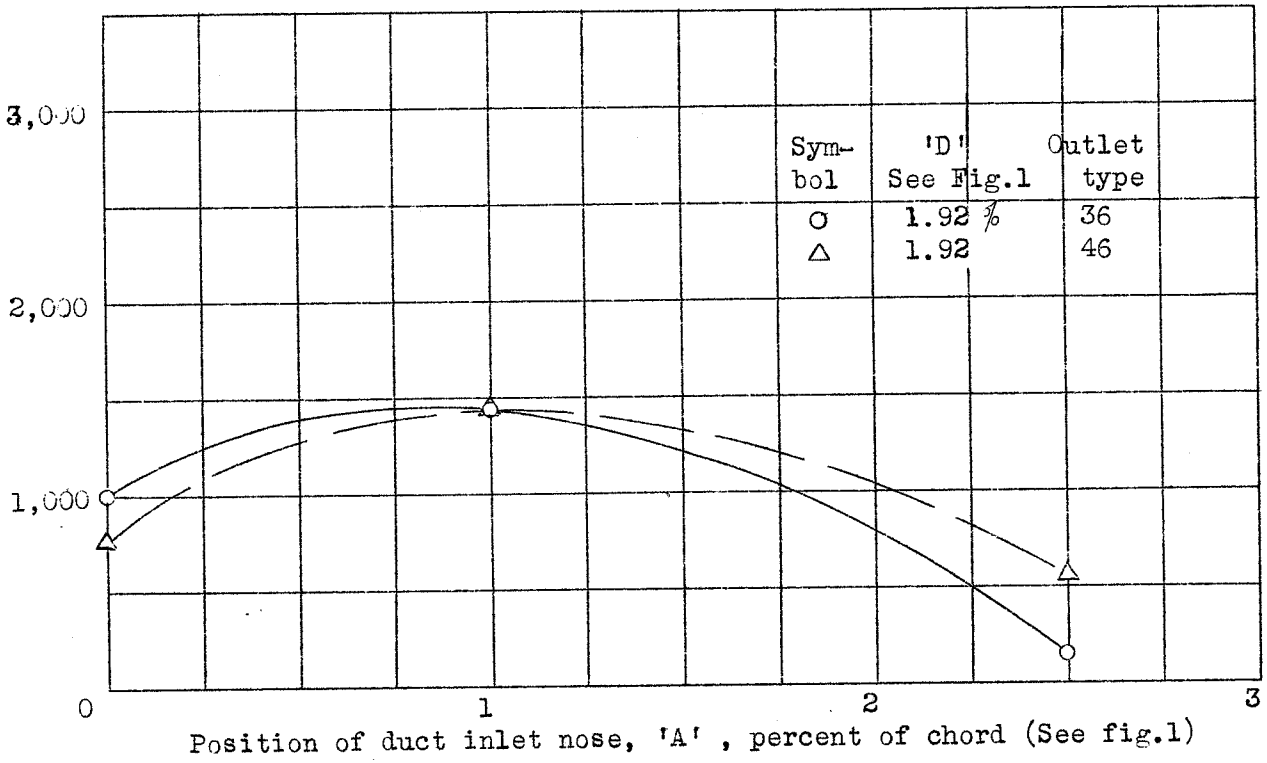

Figure 14. - Variation in air flow with the position of the duct inlet nose.
Test velocity = 100 m.p.h. Lift coefficient = 0.15

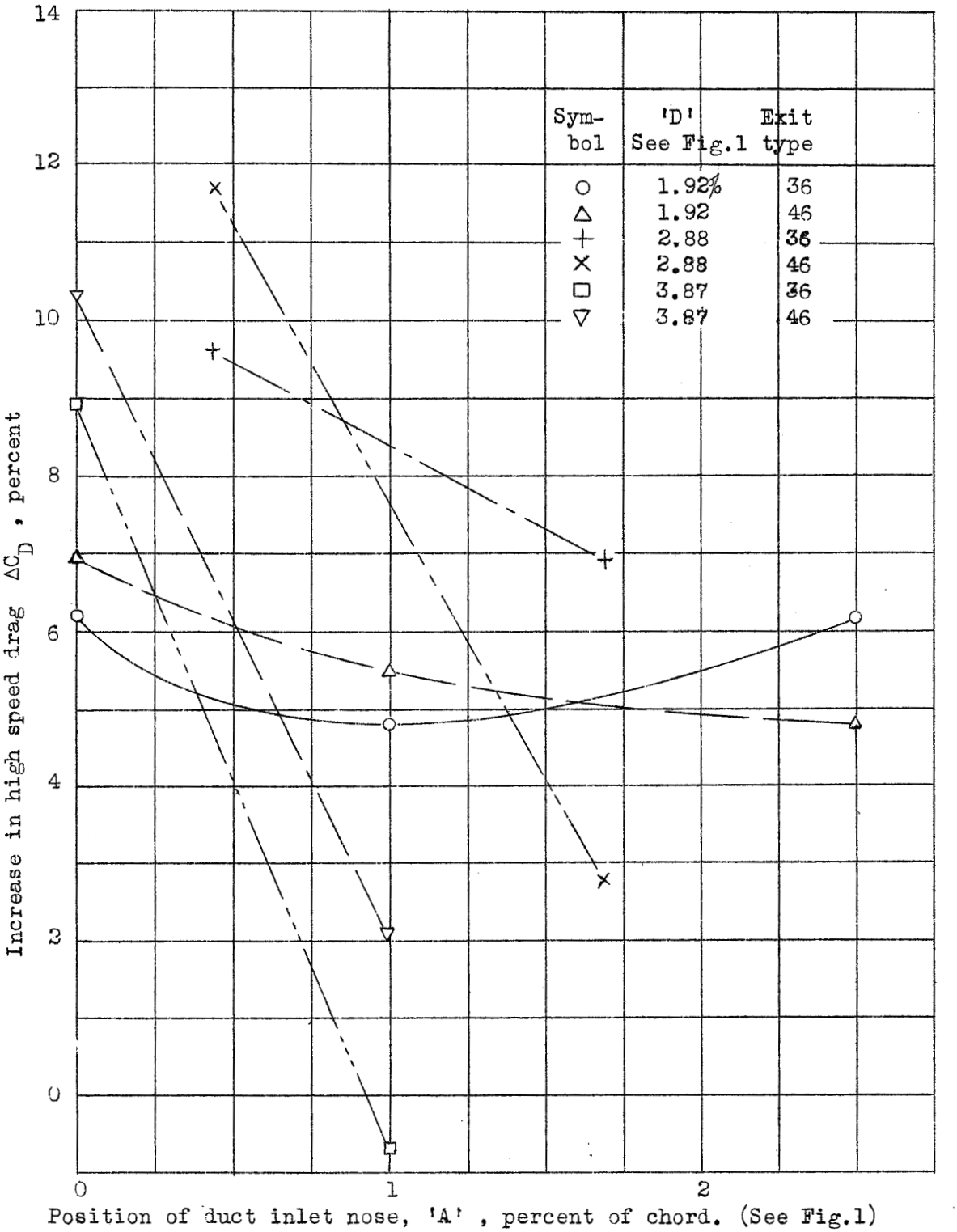

Figure 15. - Effect of inlet nose position on high speed drag. Test velocity = 60 m.p.h. Arrangement 'A'. Lift coefficient = 0.15

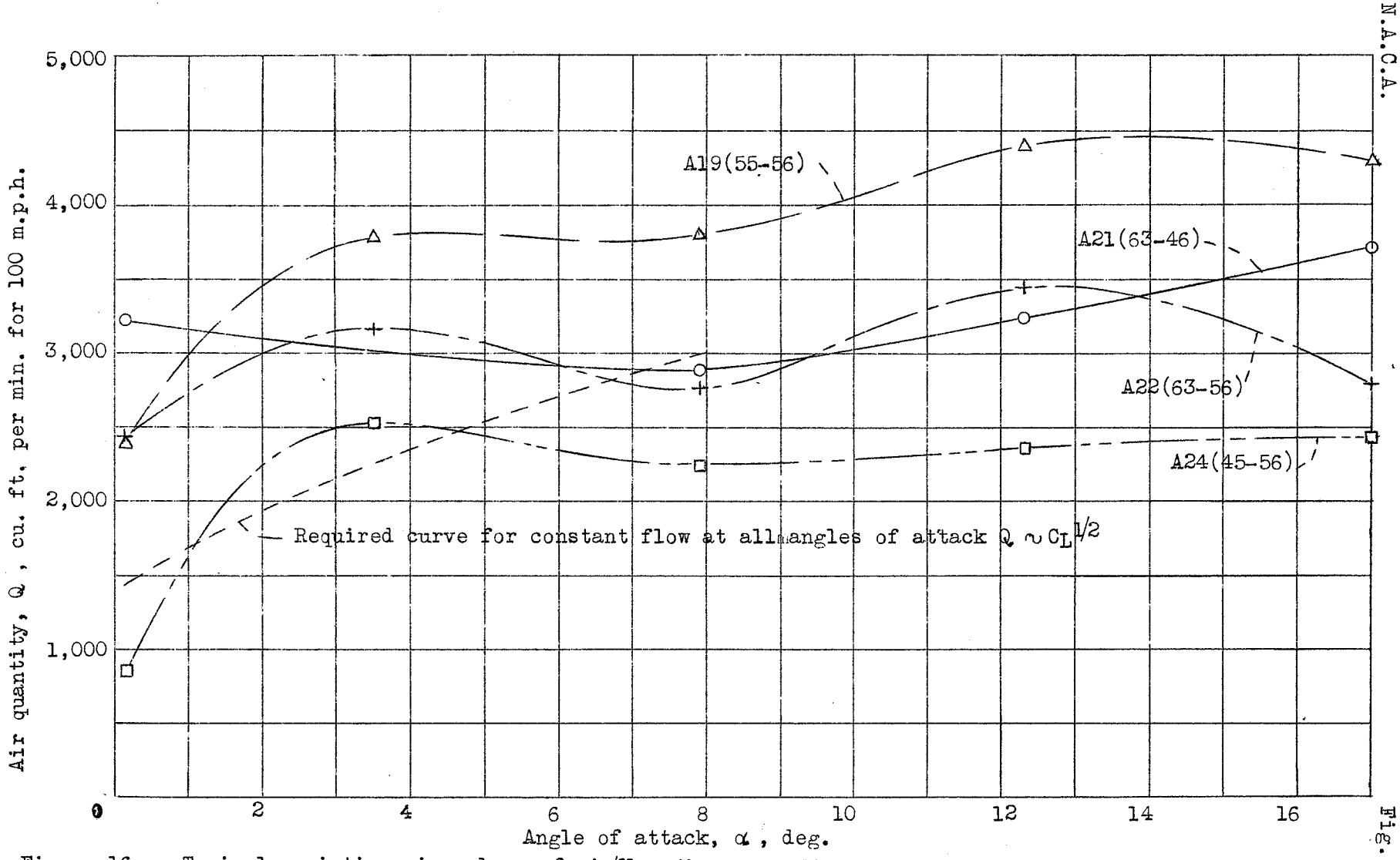

Figure 16. - Typical variations in volume of airflow through radiator ducts with angle of attack. Combinations as shown. Corrected for wind-tunnel effects.

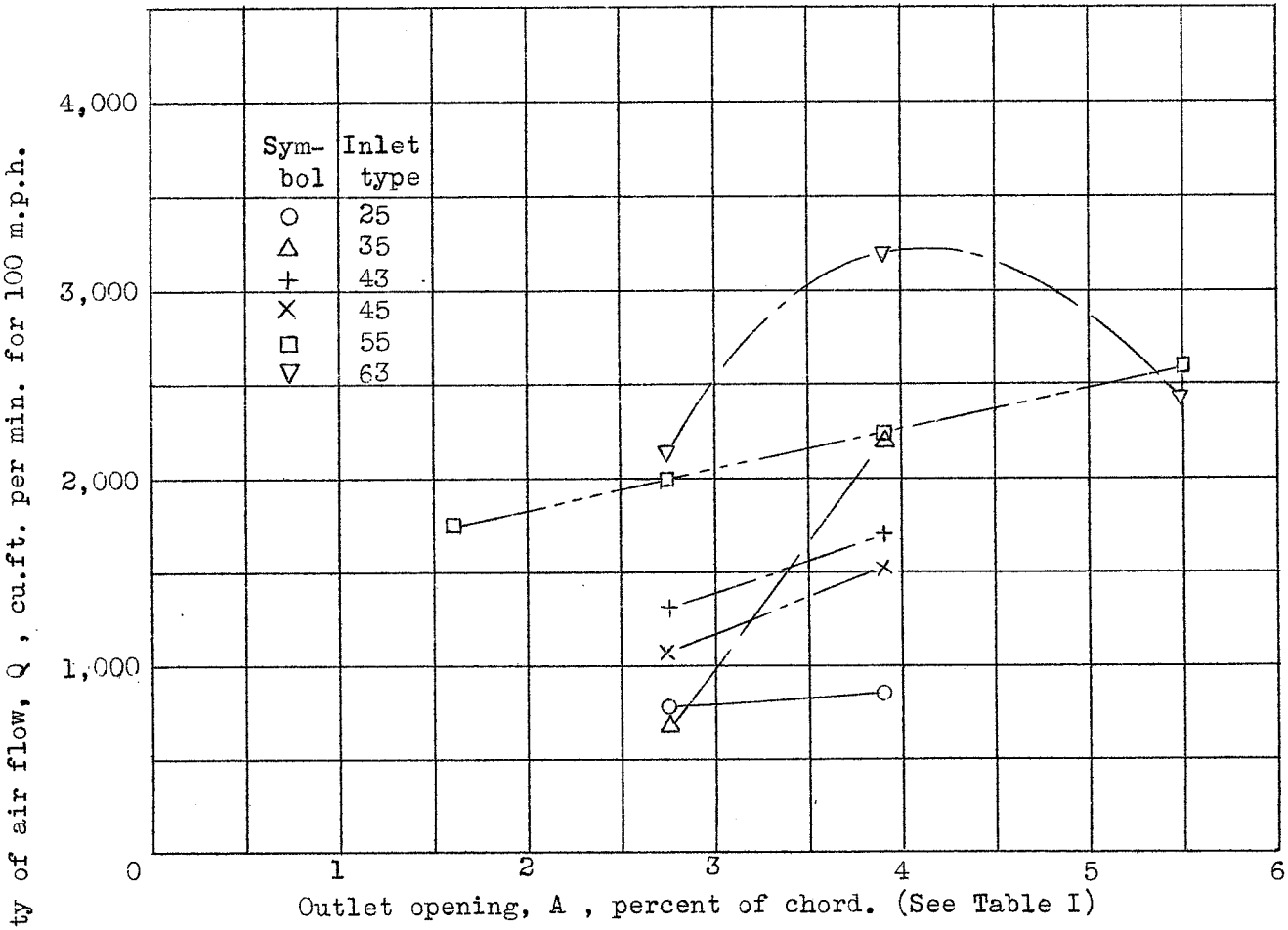

Figure 17. - Effect of outlet opening size on air flow. Test velocity = 60 m.p.h. Lift coefficient = 0.15. Test arrangement 'A'

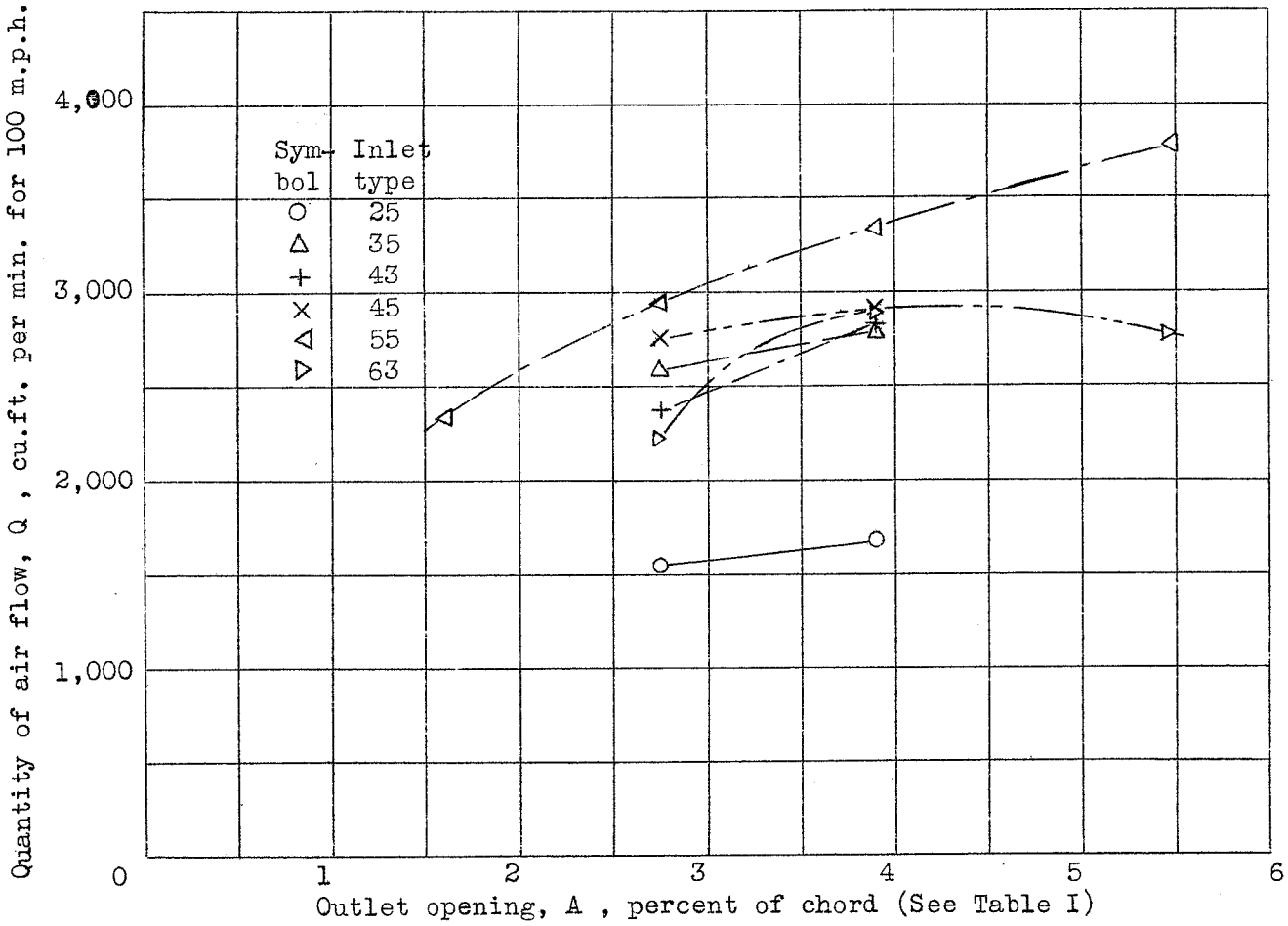

Figure 18. - Effect of outlet opening size on air flow. Test velocity =60 m.p.h. Lift coefficient = 0.70. Test arrangement 'A' .

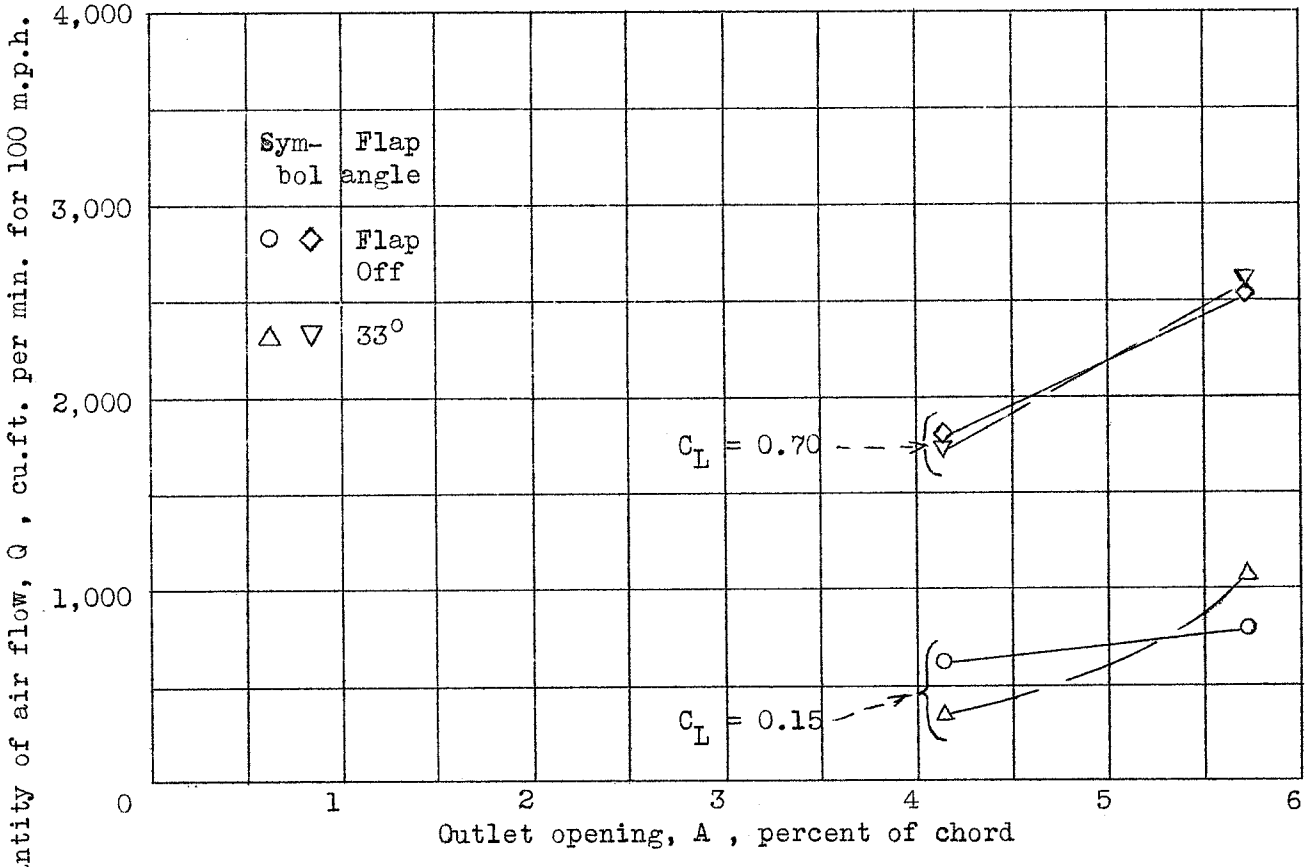

Figure 19. - Effect of outlet opening size on air flow. Test velocity = 60 m.p.h. Test arrangements 'J' & 'M'. Prestone radiator only.

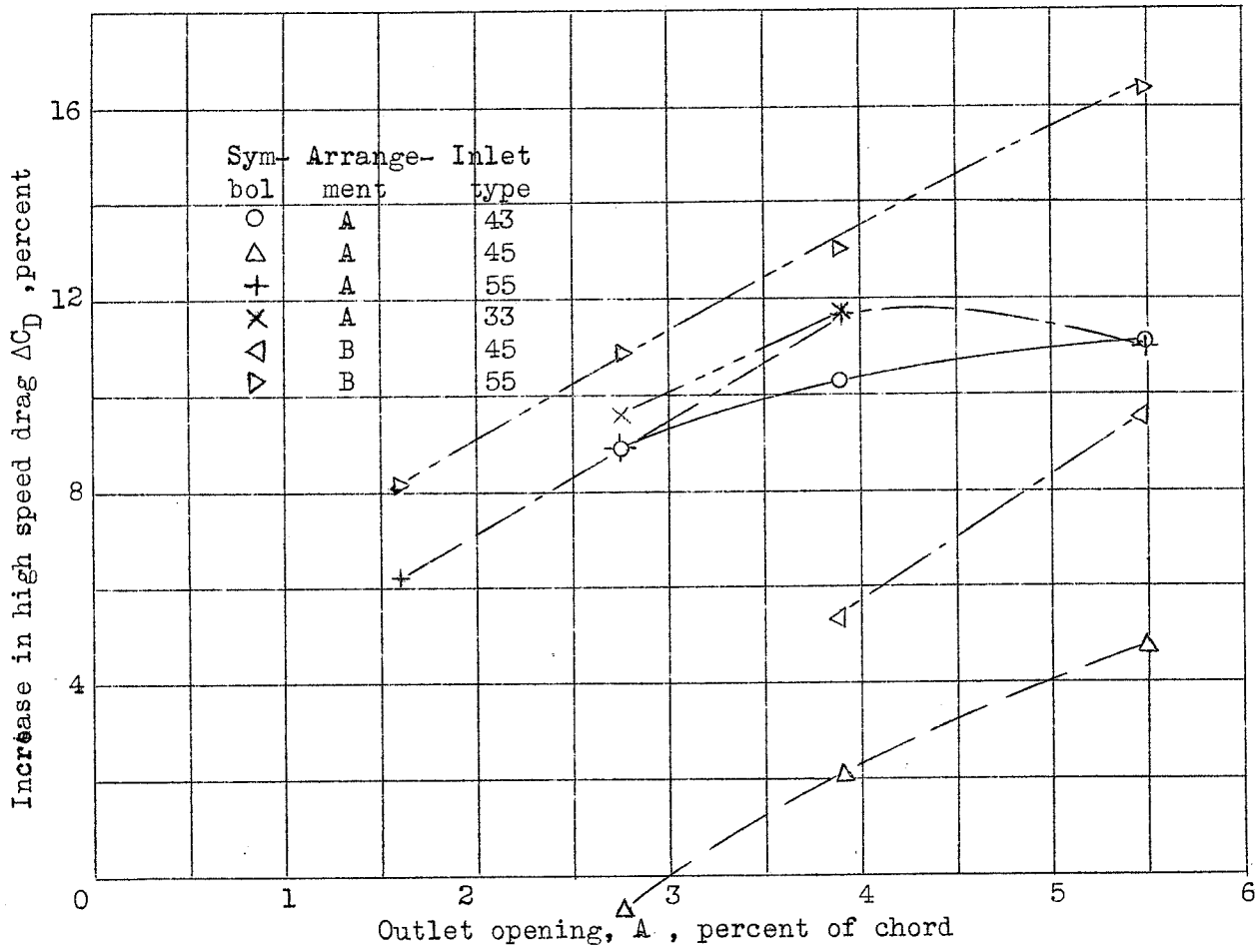

Figure 20. - Effect of outlet opening size on high speed drag. Test velocity = 60 m.p.h. Lift coefficient = 0.15

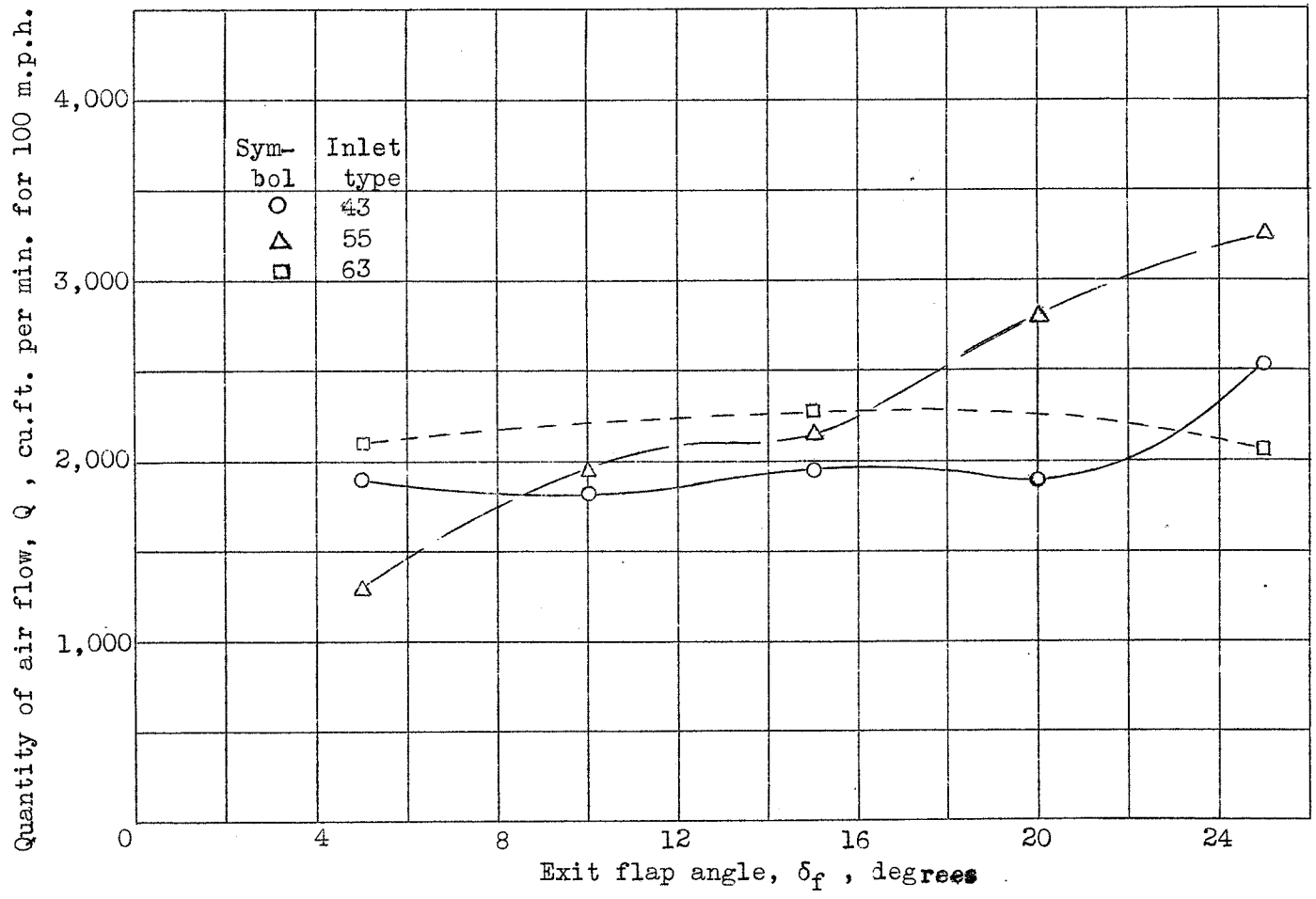

Figure 21. - Effect of flap angle on air flow. Test arrangement 'G'. Test velocity = 60 m.p.h. Lift coefficient = 0.15

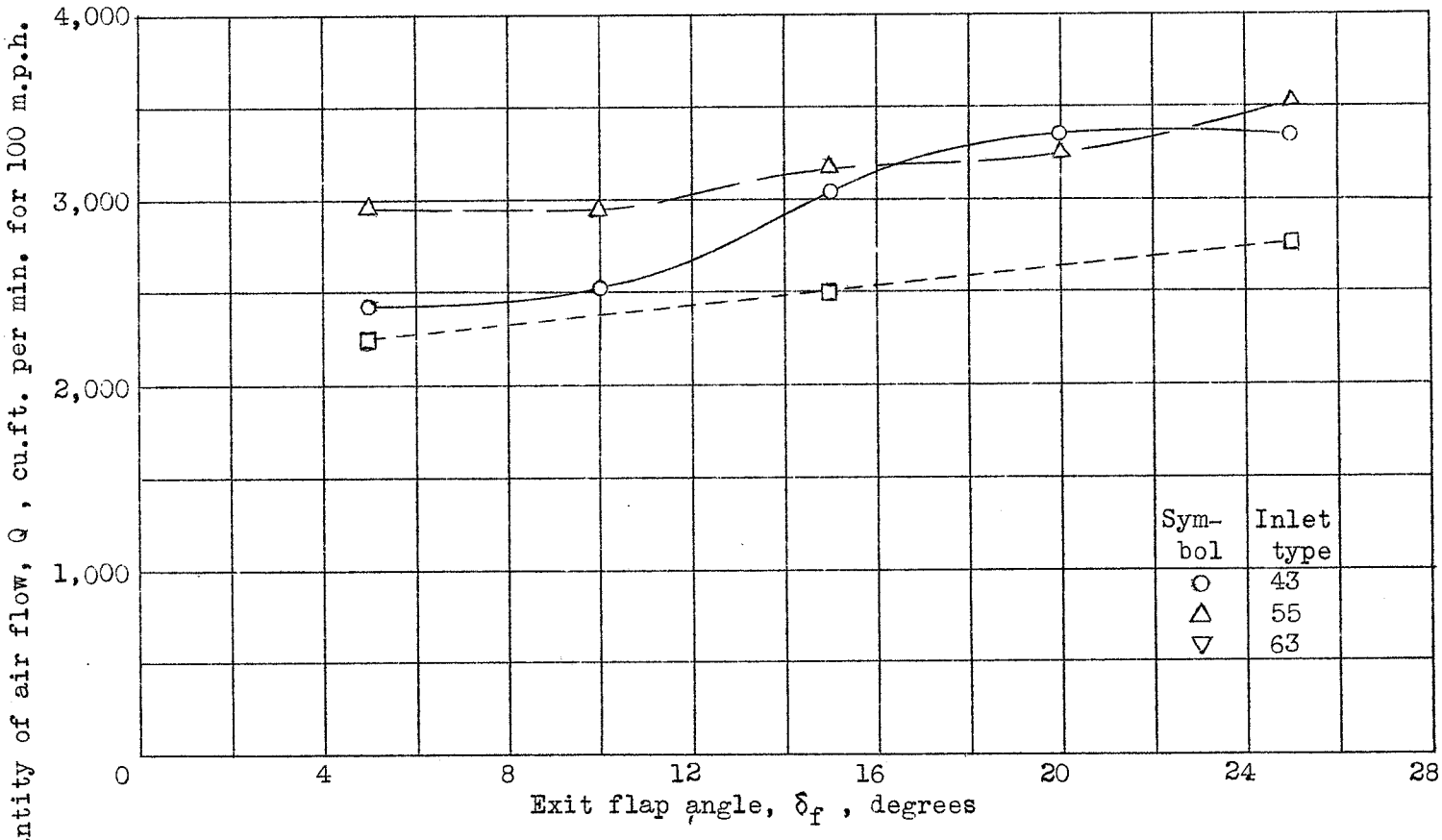

Figure 22. - Effect of flap angle on air flow. Test arrangement 'G'. Test velocity = 60 m.p.h. Lift coefficient = 0.70 .

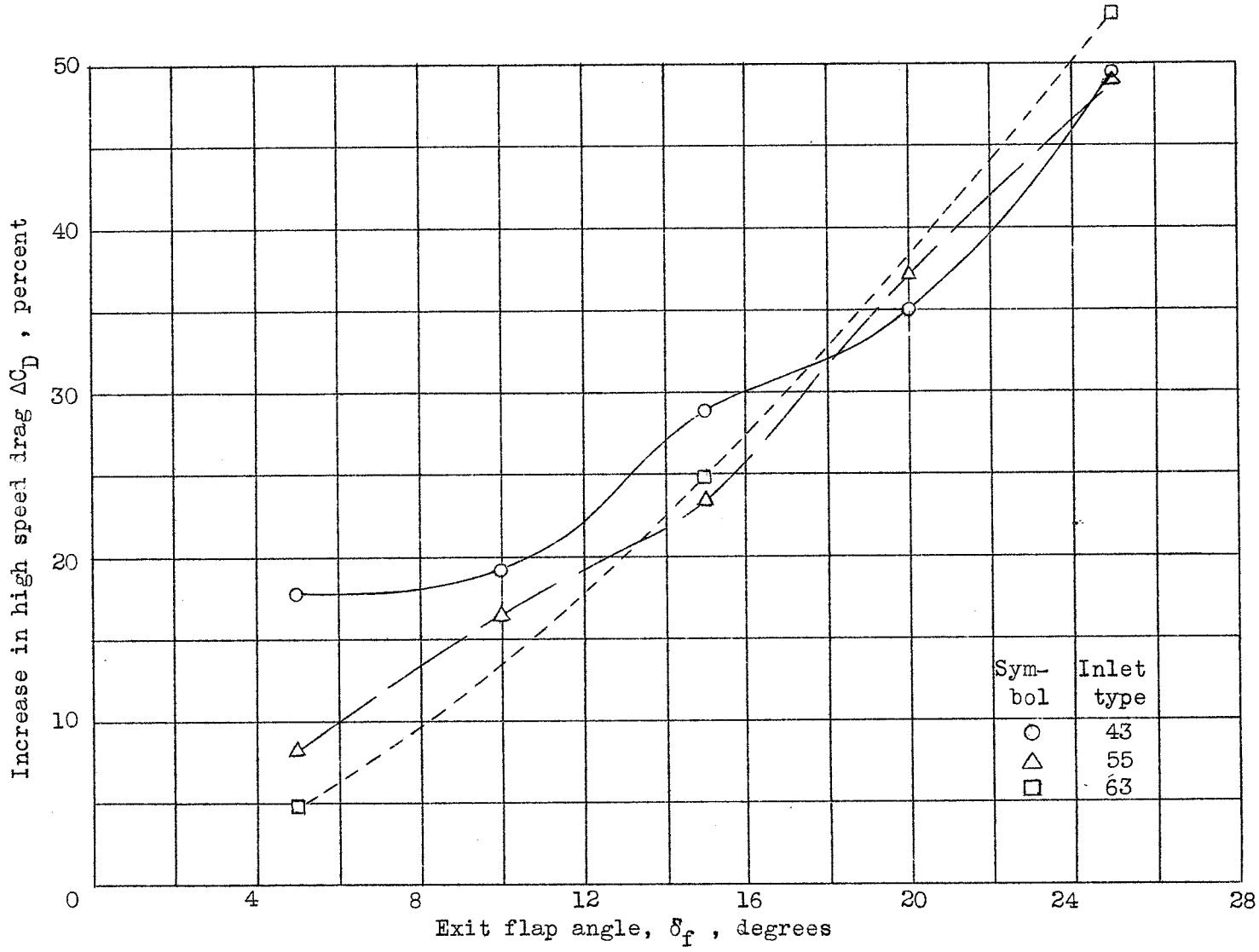

Figure 23. - Effect of flap angle on high speed drag. Test arrangement 'G'. Test velocity = 60 m.p.h. Lift coefficient = 0.15

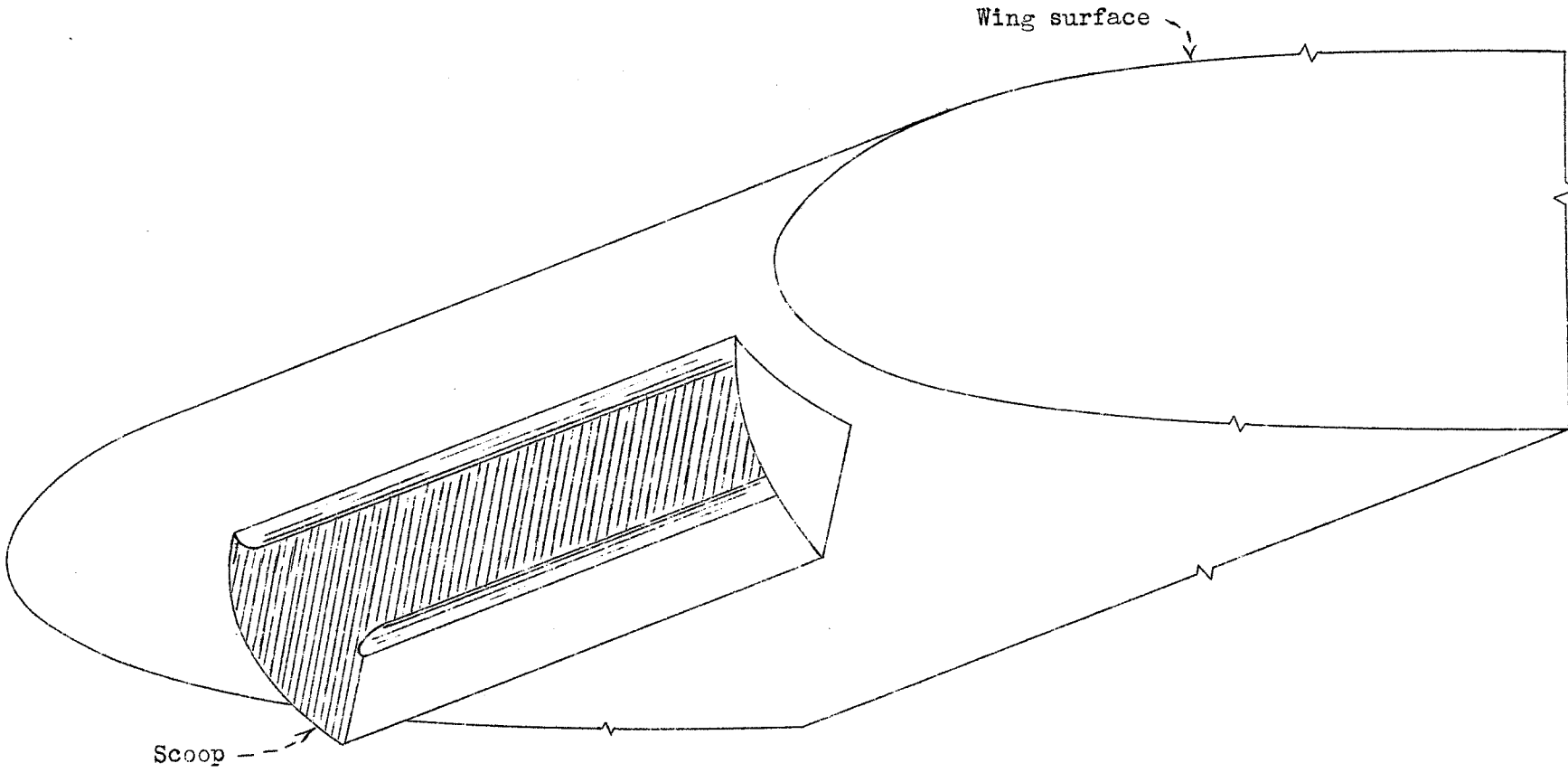

Figure 24. - Typical nose scoop installation

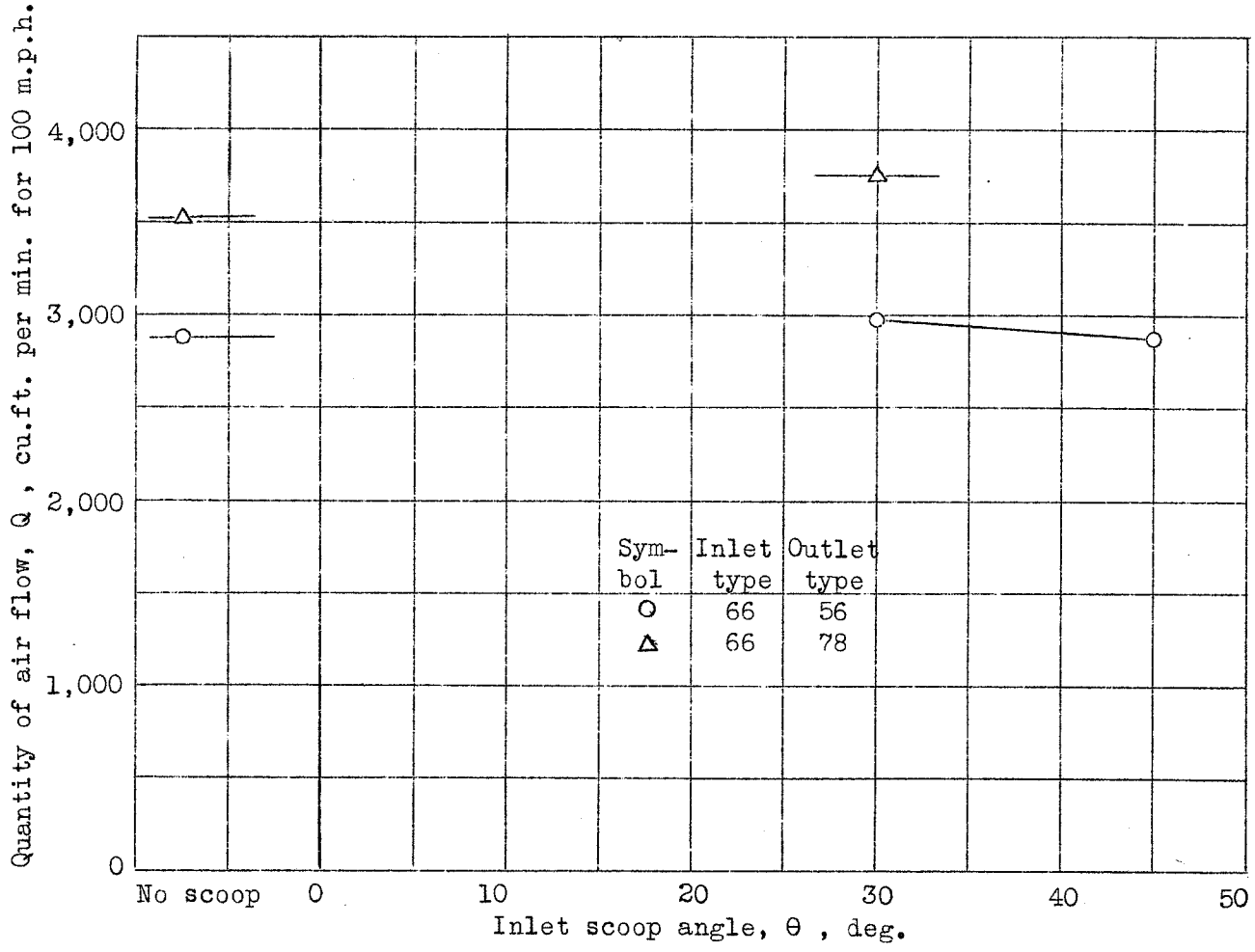

Figure 25. - Effect of inlet scoops on air flow. Test velocity = 60 m.p.h. Lift coefficient = 0.70. Test arrangement 'I' .

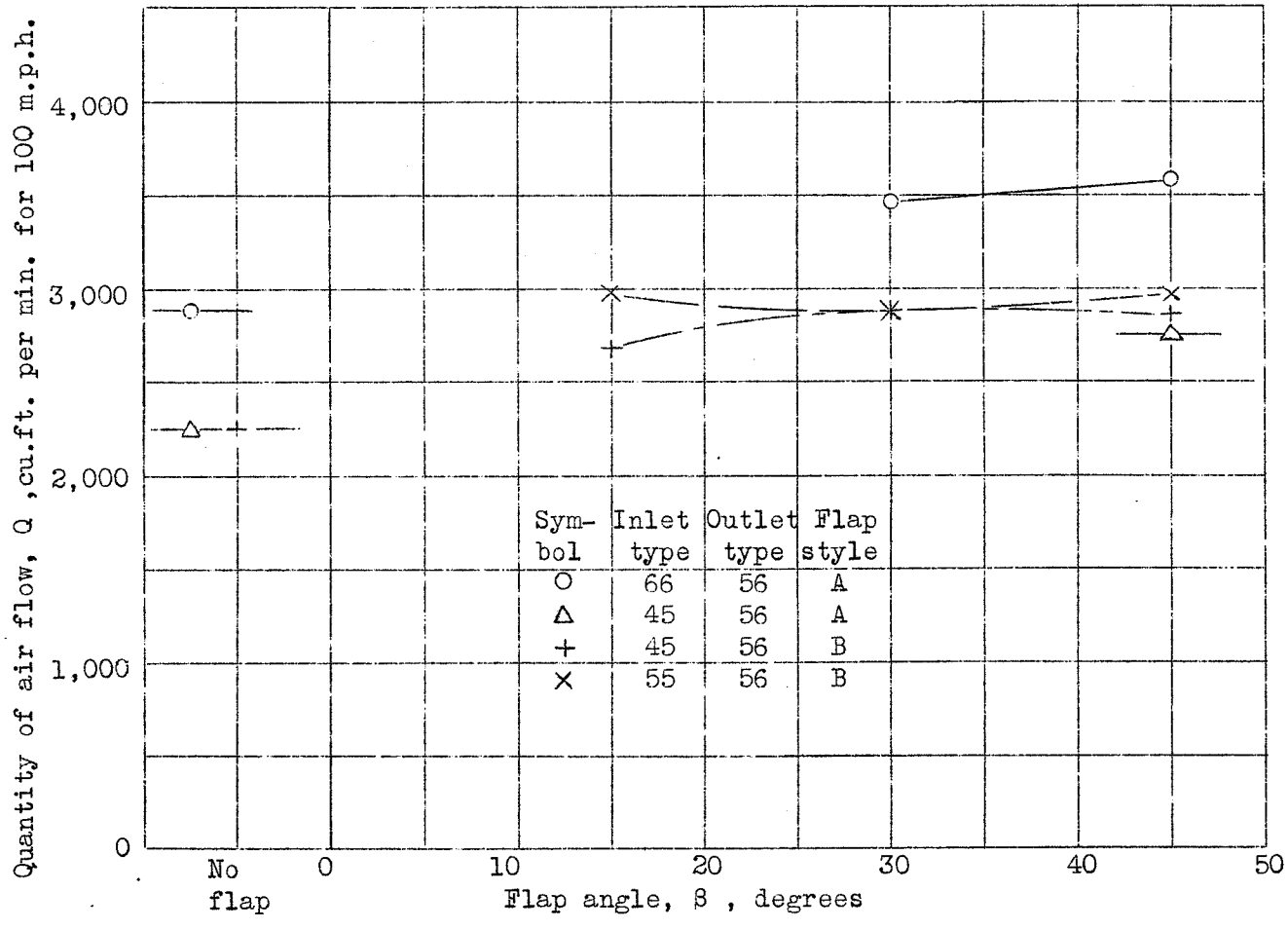

Figure 26. - Effect of exit flaps on air flow. Test velocity = 60 m.p.h. Lift coefficient = 0.70 . Test arrangement 'H' .

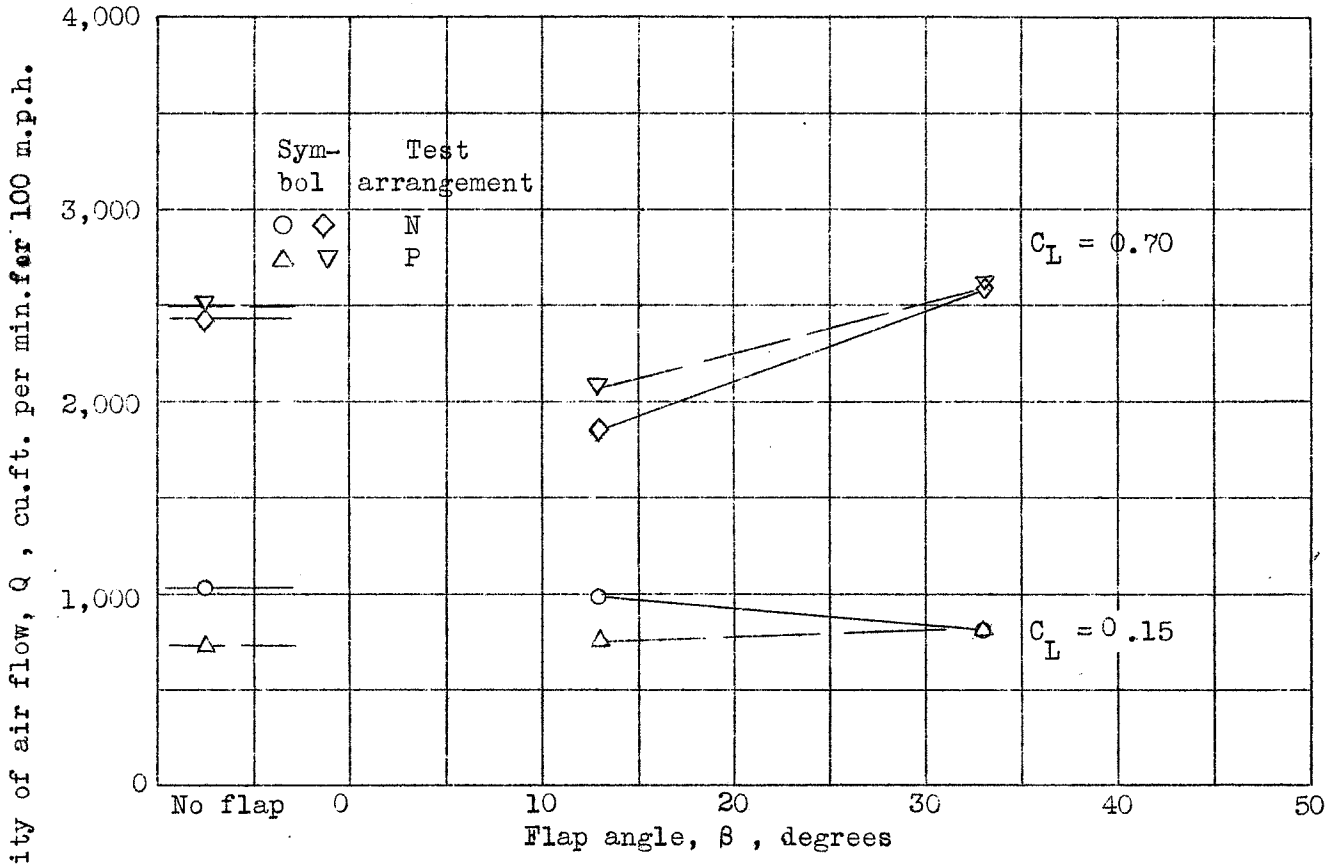

Figure 27. - Effect of exit flaps on airflow. Test velocity = 60 m.p.h.

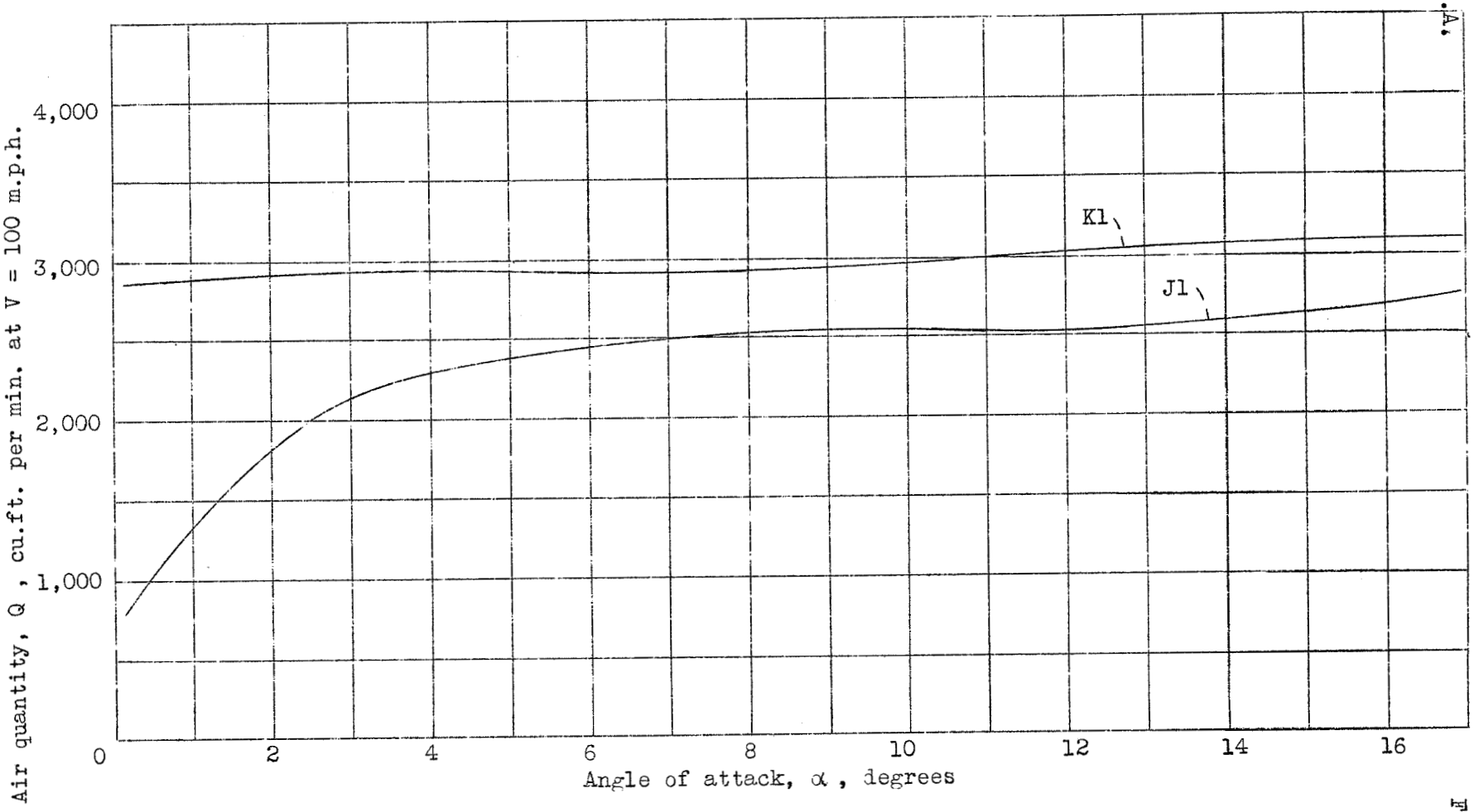

Figure 28. - Sample variations in volume of air flow through radiator ducts with angle of attack. Combinations as shown. Corrected for wind-tunnel effect.